PLOS PATHOGENS

RESEARCH ARTICLE

Berberine governs NOTCH3/AKT signaling to enrich lung-resident memory T cells during tuberculosis

Isha Pahuja[1,2☯], Kriti Negi[1☯], Anjna Kumari[1], Meetu Agarwal[2], Suparba Mukhopadhyay[1], Babu Mathew[3], Shivam Chaturvedi[1], Jaswinder Singh Maras[3], Ashima Bhaskar[1]*, Ved Prakash Dwivedi[1]*

1 Immunobiology Group, International Centre for Genetic Engineering and Biotechnology, Aruna Asaf Ali Marg, New Delhi, India, **2** Department of Molecular Medicine, Jamia Hamdard University, New Delhi, India, **3** Department of Molecular and Cellular Medicine, Institute of Liver and Biliary Sciences, New Delhi, India

☯ These authors contributed equally to this work.
* ashimabhaskar23@gmail.com (AB); vedprakashbt@gmail.com (VPD)

Citation: Pahuja I, Negi K, Kumari A, Agarwal M, Mukhopadhyay S, Mathew B, et al. (2023) Berberine governs NOTCH3/AKT signaling to enrich lung-resident memory T cells during tuberculosis. PLoS Pathog 19(3): e1011165. https://doi.org/10.1371/journal.ppat.1011165

Editor: David M. Lewinsohn, Portland VA Medical Center, Oregon Health and Science University, UNITED STATES

Received: October 11, 2022

Accepted: January 30, 2023

Published: March 7, 2023

Data Availability Statement: The authors confirm that all data underlying the findings are fully available without restriction. All relevant data are within the paper and its Supporting Information files.

Funding: IP is the recipient of Junior Research Fellowship from HGK-IYBA grant provided by the Department of Biotechnology Government of India. AK is the recipient of Senior Research Fellowship from University Grants Commission, Government

Abstract

Stimulation of naïve T cells during primary infection or vaccination drives the differentiation and expansion of effector and memory T cells that mediate immediate and long-term protection. Despite self-reliant rescue from infection, BCG vaccination, and treatment, long-term memory is rarely established against *Mycobacterium tuberculosis* (*M.tb*) resulting in recurrent tuberculosis (TB). Here, we show that berberine (BBR) enhances innate defense mechanisms against *M.tb* and stimulates the differentiation of Th1/Th17 specific effector memory (T_{EM}), central memory (T_{CM}), and tissue-resident memory (T_{RM}) responses leading to enhanced host protection against drug-sensitive and drug-resistant TB. Through whole proteome analysis of human PBMCs derived from PPD^+ healthy individuals, we identify BBR modulated NOTCH3/PTEN/AKT/FOXO1 pathway as the central mechanism of elevated T_{EM} and T_{RM} responses in the human $CD4^+$ T cells. Moreover, BBR-induced glycolysis resulted in enhanced effector functions leading to superior Th1/Th17 responses in human and murine T cells. This regulation of T cell memory by BBR remarkably enhanced the BCG-induced anti-tubercular immunity and lowered the rate of TB recurrence due to relapse and re-infection. These results thus suggest tuning immunological memory as a feasible approach to augment host resistance against TB and unveil BBR as a potential adjunct immunotherapeutic and immunoprophylactic against TB.

Author summary

In response to primary infections or vaccination, the host immune system elicits robust effector and memory responses to facilitate immediate pathogen clearance and to establish long-term protection. In this study, we have ascertained the prospects of potent immunomodulator berberine (BBR) in instigating host protective immunological memory responses during tuberculosis (TB). BBR-induced glycolytic flux stimulates pro-

of India. KN is the recipient of Junior Research Fellowship from Indian Council of Medical Research, Government of India. AB is the recipient of DST-INSPIRE Faculty Fellowship, Department of Science and Technology, Government of India and HGK-IYBA Fellowship from Department of Biotechnology, Government of India. VPD is also a recipient of DST-INSPIRE Faculty Fellowship, Department of Science and Technology, Government of India and an Early Career Research Award from Science and Engineering Research Board (SERB), Department of Science and Technology, Government of India. We would also like to acknowledge the funding support from Science and Engineering Research Board (SERB), Department of Science and Technology, Government of India and ICGEB, New Delhi, India. The funders had no role in study design, data collection and analysis, decision to publish, or preparation of the manuscript.

Competing interests: The authors have declared that no competing interests exist.

inflammatory immune responses against Mycobacterium tuberculosis (*M.tb*). BBR further prompted NOTCH-mediated AKT inhibition and activation of FOXO1, STAT3, STAT4, BLIMP-1, and NFκB signaling thereby enriching *M.tb*-specific resident memory T cell population in the distinct murine TB disease models and human CD4+ T cells. These results project BBR as an adjunct immunotherapeutic and immunoprophylactic against TB.

Introduction

In spite of being avertable and treatable, tuberculosis (TB) caused by *Mycobacterium tuberculosis* (*M.tb*) is the major cause of mortality and morbidity among infectious diseases. Globally 10 million people were diseased with TB and an aggregate of 1.3 million people passed away in 2020 itself [1]. Furthermore, almost one-fourth of humankind is infected asymptomatically (latently) with *M.tb*, with a 5–15% risk of progressing into clinical manifestations [1].

Existing anti-tubercular treatment (ATT) comprising of assorted anti-mycobacterial drugs can only exterminate active, drug-sensitive strains of *M.tb*. However, failure to complete the extensive TB restraint approach, directly observed treatment short-course (DOTS) frequently brings about the emergence of multi-drug resistant (MDR) and extensively-drug resistant (XDR) strains. Moreover, DOTS therapy instigates severe toxicity and impairment of host immune responses. For instance, isoniazid (INH) usage leads to the cessation of antigen-responding $CD4^+$ T lymphocytes, which results in a heightened risk of reactivation and reinfection with *M.tb* [2]. Further inefficacy of the only available vaccine *M. bovis* bacille Calmette-Guérin (BCG) to prevent adult pulmonary TB makes it a requisite to employ appropriate strategies to augment the host control of *M.tb* infection [3].

Subsequent to infection, *M.tb* is phagocytosed by antigen-presenting cells (APCs) that participate in the extermination of internalized pathogens, promote activation of T lymphocytes and stimulate protective pro-inflammatory cytokines such as IFNγ and IL17 [4–6]. The immunological response in TB is extremely complex and the fate of infection is governed predominantly by subsets of T lymphocytes [7]. For instance, stimulation of T helper 2 (Th2) cells and regulatory T cells (Tregs) result in the advancement of disease by hampering protective Th1 responses [8,9,10] while Th1/Th17subsets are associated with host protective immune responses [11]. Nonetheless, these cytokine responses decline post *M.tb* clearance and hence, subsets of memory T cells play a crucial role in providing long-term protection in TB [11]. T cell receptor (TCR) signaling following antigen stimulation along with cytokine environment regulates and shapes host memory responses [12]. Sustained AKT activation following TCR stimulation drives terminal T cell differentiation [13] probably by targeting FOXO proteins [14,15]. JAK/STAT pathways also influence the differentiation of naïve T cells into memory subsets [16]. Further, STAT4 and Blimp1 transcription factors are known to regulate resident memory responses at the local site of infection. T effector memory (T_{EM}) cells provoke Th1 type cytokines and protect against acute *M.tb* infections whereas, T central memory (T_{CM}) can give rise to T_{EM} during disease progression, direct cell-mediated immunity for bacterial clearance and sustain long-term memory responses [17,18]. Hence, a strengthened T_{CM} and T_{EM} population is vital for the continuation of long-term protective immune responses [19]. Apart from these, tissue-resident memory T cells (T_{RM}) localized at distinctive sites of infections like lung and spleen are linked with positive medical consequences and host protective responses [20].

Mostly host immune responses elicited in response to *M.tb* can successfully contain pathogen [4] but complete sterility is not attained. Hence, a novel immunomodulatory approach is

necessitated to boost current therapeutics to ease up drug regimen, lessen therapy-induced adversities and intensify anti-mycobacterial effects [21,22,23]. BBR ($C_{20}H_{18}NO_4^+$) a bioactive isoquinoline alkaloid is known for diverse therapeutic effects. Administering BBR adjunct to therapeutics can induce hepatoprotective effects by modulating inflammatory responses [24]. BBR can induce protection against INH-associated inflammation, oxidative stress and liver damage in rats [25]. BBR has shown affirmative outcomes *in vitro* against clinical drug-resistant bacterial strains [26], and *in vivo* against drug-sensitive *M.tb* with limited insight into the mechanism of protection[27]. In this study, we have investigated the anti-mycobacterial potential of BBR against pathogenic laboratory strain H37Rv and drug-resistant clinical isolates of *M.tb ex vivo* and in the murine model of TB. We observed that BBR significantly lowered the bacterial burden in the lungs and the spleen of *M.tb* infected mice in solitary or in combination with the first-line anti-TB drug INH primarily by boosting the protective host immune responses such as macrophage activation, Th1/Th17 polarization, memory T cell enhancement and pro-inflammatory cytokine responses. NOTCH mediated AKT inhibition and activation of FOXO1, STAT3, STAT4, BLIMP-1 and NFκB signaling following BBR treatment led to a profound induction of adaptive memory in human $CD4^+$ T cells and in mice model. These immunomodulatory properties of BBR were also exploited to increase the vaccine efficacy of BCG. Furthermore, induction of superior memory responses significantly lowered the recurrence of TB due to re-activation and re-infection. Overall, these results propound BBR as an attractive adjunct immunotherapeutic and immunoprophylactic against TB.

Results

BBR enhances host resistance against drug-susceptible and drug-resistant strains of *M.tb*

Numerous studies have evaluated the therapeutic potential of BBR against diverse ailments. However, the effectiveness of BBR against *M.tb* infection is yet to be uncovered. Since BBR has been shown to possess weak anti-bacterial activity [28], we foremost aimed to determine its anti-mycobacterial activity against different drug-sensitive and -resistant strains of *M.tb*. Consistent with the previous studies, BBR displayed bacterial toxicity at $\leq$ 50 μg/ml against all the strains tested (**S1A–S1C Fig**) however 20 μg/ml of BBR treatment which displayed no toxicity in the mouse peritoneal macrophages (**S1D and S1E Fig**) significantly decreased the intracellular *M.tb* growth (**Fig 1A**) indicating the immunomodulatory effects of BBR on host macrophages. With no variable effect on ROS generation (**S1F and S1G Fig**), BBR treatment significantly induced apoptosis in uninfected (**S1H Fig**) and *M.tb* infected macrophages (**Fig 1B and 1C**) and led to significant activation of transcription factors (NFkB and STAT3) which play a crucial role in combating TB (**Fig 1D**)**.** Further, BBR treatment significantly enhanced the expression of CD11b and co-stimulatory molecules CD40 and CD86 on the surface of infected macrophages (**Fig 1E–1G**). Moreover, BBR treated macrophages also displayed increased expression of M1 specific pro-inflammatory cytokines (**Fig 1H**). Furthermore, immunomodulatory effect of BBR was consistent in T cells isolated from infected mice wherein the percentage of $CD69^+$ activated $CD4^+$ T lymphocytes was significantly enriched upon BBR treatment (**Fig 1I**). Co-culturing infected macrophages with BBR primed T cells demonstrated significantly reduced intracellular bacterial burden (**Fig 1J and 1K**) as compared to infected macrophages as well as untreated T cells co-cultured with macrophages. Few piecemeal studies have reported BBR as an efflux pump inhibitor and thereby is known to increase the intracellular concentration of the antibiotics [29]. We investigated whether BBR co-treatment increased the killing potential of INH. With no significant effect *in vitro* (**S1G Fig**) BBR

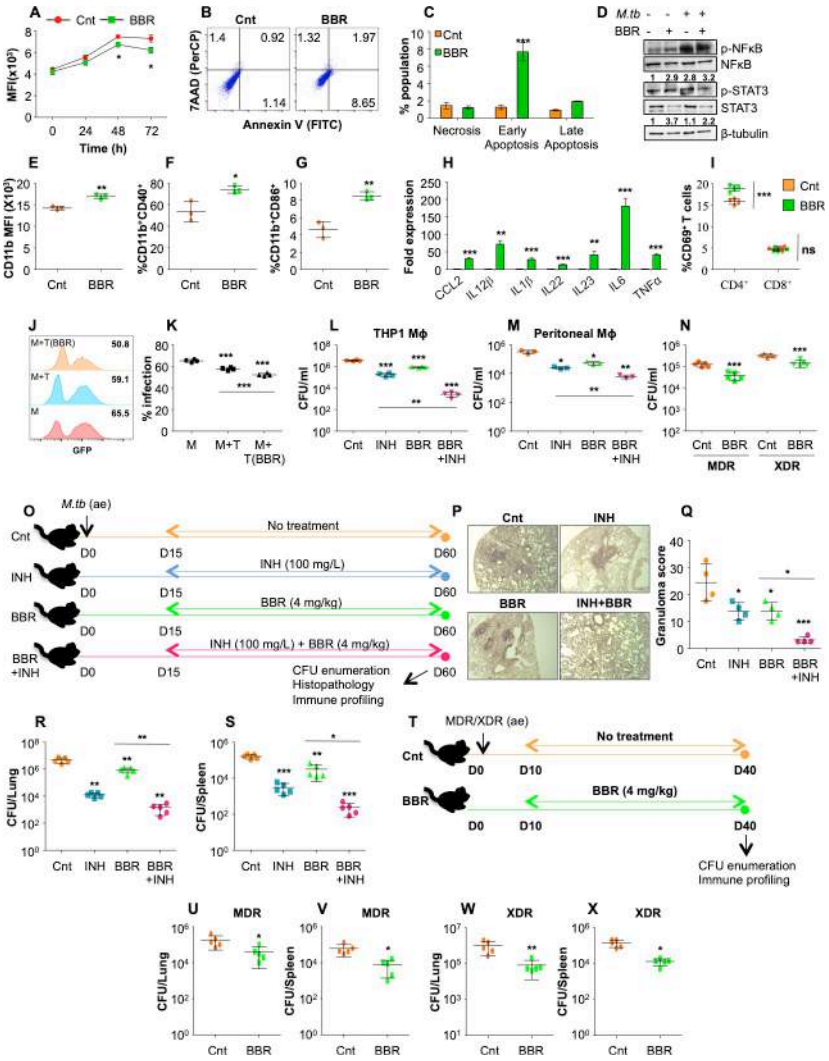

Fig 1. BBR treatment enhances host resistance against drug-sensitive and drug–resistant TB. (A) Mouse peritoneal macrophages were infected with GFP expressing H37Rv (Rv-GFP) at 1:10 MOI followed by treatment with BBR (20 μg/ml). At different time points, cells were analysed by flow cytometry. Graph represents the GFP fluorescence at indicated time points with and without BBR treatment. **(B-C)** Mouse peritoneal macrophages were infected with *M.tb* at MOI of 1:10 followed by treatment with BBR (20 μg/ml) for 48 h followed by apoptosis analysis via flow cytometry. **(B)** Representative dot plots and **(C)** Percentage of apoptotic cells with and without BBR (20μg/ml) treatment. **(D)** Immunoblots depicting the phosphorylation of indicated transcription factors (NFkB and STAT3) in uninfected and infected mouse peritoneal macrophages with or without BBR treatment. **(E-G)** Infected murine peritoneal macrophages were surface stained with antibodies against CD11b (APC/Cy7), CD40 (PE) and CD86 (PerCPCy5.5) followed by flow cytometry. **(E)** Expression of CD11b on the surface of infected macrophages. Percentage of **(F)** $CD11b^{+}CD40^{+}$ and **(G)** $CD11b^{+}CD86^{+}$ infected macrophages with and without BBR treatment. **(H)** Expression of chemokines and cytokines in *M.tb* infected macrophages at 24h pi with and without BBR (20 μg/ml) treatment. **(I)** Percentage of $CD4^{+}$ and $CD8^{+}$ T cells expressing CD69 in the infected and BBR (10μg/ml) treated splenocytes. **(J)** Representative overlay plots and **(K)** percentage of RvGFP infected macrophages co-cultured with *M.tb* specific and BBR treated splenocytes. **(L)** PMA- activated THP1 macrophages were infected with H37Rv at 1:10 MOI followed by treatment with INH (1 μg/ml), BBR (20 μg/ml) or both for 48 h pi after which cells were lysed for CFU enumeration. **(M)** Experiment L was repeated in mouse peritoneal macrophages. **(N)** Mouse peritoneal macrophages were infected with MDR (Jal 2261) and XDR (MYC431) clinical strains of *M.tb* followed by treatment with 20 μg/ml of BBR. Cell lysates were plated for CFU enumeration 48 h pi. **(O)** Schematic representation of the murine model of infection. C57BL/6 mice were infected with low dose of H37Rv (~110 CFU per lung) and after 15 days of disease establishment, mice were treated with either INH (100 mg/L), BBR (4 mg/kg) or both for 45 days followed by CFU enumeration and immune profiling. **(P)** Histopathology of infected lungs with arrows indicating the granulomatous lesions. **(Q)** Immunopathology score of the infected lungs. Bacterial burden in the **(R)** lungs and the **(S)** spleen of infected animals. **(T)** Diagrammatic representation of the infection model. Bacterial burden in **(U)** the lungs and **(V)** the spleen of mice

infected with MDR strain of *M.tb*. Bacterial load in **(W)** the lungs and **(X)** the spleen of mice infected with XDR strain of *M.tb*. Data is representative of two independent experiments. The data values represent mean ± SD (n = 3–5). $^{*}p<0.05$, $^{**}p<0.005$, $^{***}p<0.0005$.

https://doi.org/10.1371/journal.ppat.1011165.g001

co-treatment significantly reduced the bacterial burden in the INH treated macrophages as compared to INH treatment alone in both human (Fig 1L) and mice derived macrophages (Fig 1M). BBR also reduced the intracellular load of MDR and XDR strains of *M.tb* (Fig 1N) emphasizing that the immunomodulatory potential of BBR is not restricted to drug-sensitive strain of *M.tb*. To further corroborate the outcomes of *ex vivo* experiments, C57BL/6 mice were infected with a low dose (∼110 CFU) of *M.tb* H37Rv and left untreated or treated with BBR (4mg/kg) either alone or in combination with INH (100mg/L) for 45 days followed by CFU enumeration and immune profiling (Fig 1O). As compared to control or INH treated infected lungs, BBR treatment significantly reduced the extent of granulomatous inflammation alone and in combination with INH (Fig 1P and 1Q). Further, BBR treatment significantly reduced the bacterial burden in the lungs and the spleen of infected mice as compared to the control group (Fig 1R and 1S). Interestingly, BBR co-treatment significantly enhanced the anti-tubercular potential of INH (Fig 1R and 1S). These results demonstrate the adjunct potential of BBR along with INH against *M.tb* H37Rv. Since drug-resistant variants are one of the major contributors of global TB pandemic, we ascertained the efficacy of BBR against MDR and XDR TB (Fig 1T). Interestingly, BBR treatment significantly lowered the bacterial burden of both the drug-resistant strains tested in the lungs and spleen of mice (Fig 1U–1X).

BBR strengthens the host protective immune responses against TB

To comprehend the immunomodulatory properties of BBR, we profiled the innate and adaptive immune cell populations driving host protection in both the lungs and the spleen of infected mice. Increased percentage of $CD11b^{+}$ and $CD11c^{+}$ cells with enhanced expression co-stimulatory molecules CD80 and CD86 was observed in the lungs (S2A–S2H Fig) and the spleen (S2I–S2P Fig) of infected mice treated with BBR indicating significant innate cell stimulation which plays a crucial role in the activation of adaptive immune responses. Although BBR treatment did not change the percentage of $CD4^{+}$ and $CD8^{+}$ T cells (Fig 2A–2C), in combination with INH, BBR convalesced INH induced reduction in percentage of $CD4^{+}$ T cells (Fig 2B) in the lungs of infected mice. BBR treatment significantly induced the activation of T cell subsets as the expression of early activation marker CD69 on these cells was significantly heightened in the lungs (Fig 2D–2F) and the spleen (S3A–S3E Fig) of infected mice.

Hence, it can be inferred that BBR treatment extensively strengthens antigen processing and presentation by APCs and consistently promotes activation of T lymphocytes to impart protection against *M.tb* infection. Furthermore, BBR treatment advanced differentiation of $CD4^{+}$ and $CD8^{+}$ into protective Th1 and Th17 subsets in the lungs of infected mice. This was evident by significant increase in IFNγ and IL17 producing T cell subsets in both the lungs (Fig 2G–2K) and the spleen (S3F–S3J Fig) of BBR and INH treated mice. Furthermore, BBR treatment considerably enriched host-protective chemokines and cytokines such as TNFα, IL1β, IL22 etc., and subsided the effect of INH induced anti-inflammatory cytokines such as IL10 and IL4 in co-treated mice (Fig 2L). We further investigated the impact of BBR treatment on the induction of prolonged immune protection, which is mediated by memory subsets of adaptive immunity. The lungs of BBR treated mice revealed high frequency of T_{CM} cells (Fig 2M–2O). Similar trend was observed in the spleen of BBR treated mice (S4A–S4C Fig). Furthermore, the percentage of resident memory T cells (T_{RM}) which evolve from disseminating effector memory T cells (T_{EM}), remain confined to the tissues and play a key role in

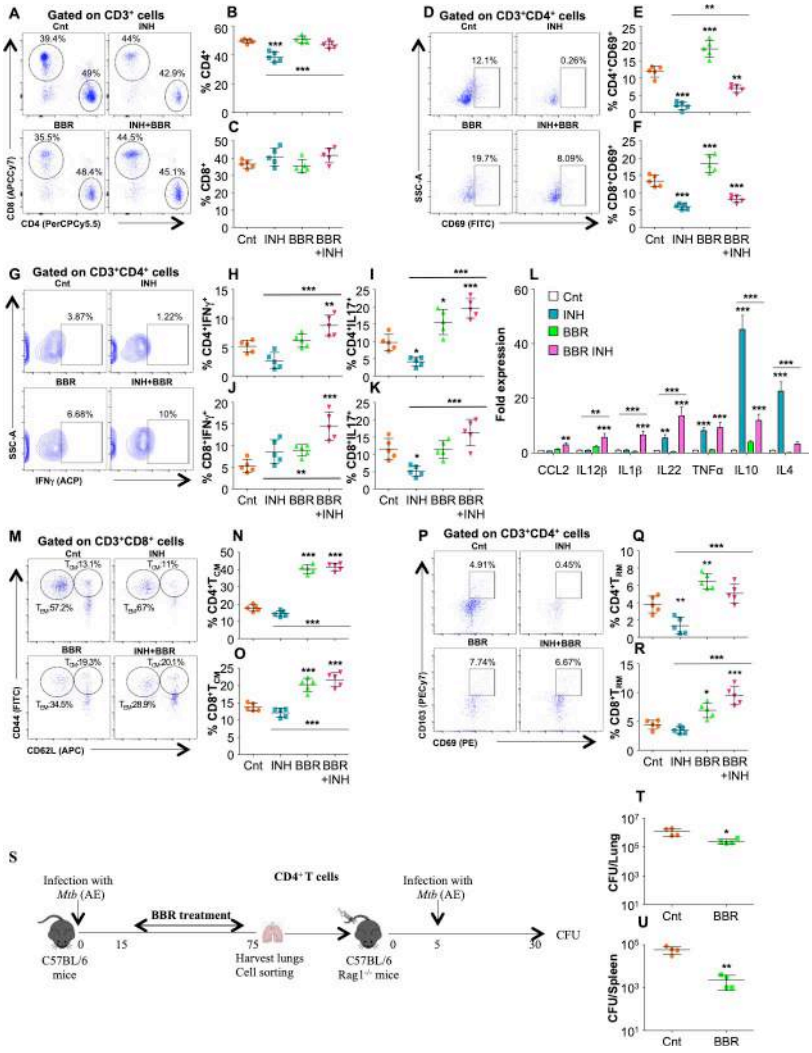

Fig 2. BBR strengthens *M.tb*-specific T cell responses during TB treatment. Single cell suspensions generated from the infected lungs were *ex vivo* stimulated with *M.tb* complete soluble antigen (CSA) for 16 h followed by surface staining with antibodies against CD3 (Pacific Blue), CD4 (PerCPCy5.5), CD8 (APCCy7) and CD69 (FITC) followed by flow cytometry. **(A)** FACS scatter dot plots and percentage of **(B)** $CD4^+$ and **(C)** $CD8^+$ T cells in the infected lungs. **(D)** Representative FACS dot plot and the percentage of **(E)** $CD4^+CD69^+$ and **(F)** $CD8^+CD69^+$ T cells in the infected lungs. **(G-K)** After stimulation with CSA, the lung cells were treated with monensin and brefeldin A for 2 h and surface stained with α-CD3 (Pacific Blue), α-CD4 (PerCPCy5.5) and α-CD8 (APCCy7) followed by intracellular staining with α-IFNγ (APC) and α-IL17 (PECy7) and flow cytometry. **(G)** Representative dot plots and percentage of **(H)** $CD4^+IFN\gamma^+$, **(I)** $CD4^+IL17^+$, **(J)** $CD8^+INF\gamma^+$ and **(K)** $CD8^+IL17^+$ cells in the infected lungs. **(L)** Fold expression of cytokines in the lungs of infected, INH and BBR treated splenocytes. **(M-R)** To determine the frequency of central memory and resident memory T lymphocytes, *ex vivo* stimulated lung cells were surface stained with α-CD3 (Pacific Blue), α-CD4 (PerCPCy5.5), α-CD8 (APCCy7), α-CD69 (PE), α-CD103 (PECy7), α-CD62L (APC) and α-CD44 (FITC) followed by flow cytometry. **(M)** Representative FACS dot plots and **(N)** the percentage of $CD4^+T_{CM}$ ($CD62L^{HI}CD44^{HI}$) cells, T cell subset. **(O)** Percentage of $CD8^+$TCM ($CD62L^{HI}CD44^{HI}$) cells, in the infected lungs with or without drug treatment. **(P)** Representative scatter dot-plot images and percentage of **(Q)** $CD4^+$TRM and **(R)** $CD8^+$TRM cells in the lungs of infected mice. **(S)** Schematic representation of adoptive transfer experiment. CFU enumeration after 21 days of adoptive transfer in **(T)** the lungs and **(U)** the spleen of Rag-/- mice. Data is representative of two independent experiments. The data values represent mean ± SD (n = 5). $^*p<0.05$, $^{**}p<0.005$, $^{***}p<0.0005$.

https://doi.org/10.1371/journal.ppat.1011165.g002

stimulating adaptive immune response at the tissue specific sites was considerably enhanced in the lungs (Fig 2P–2R) and in the spleen of infected mice (S4D–S4F Fig). Furthermore, to

strengthen our findings regarding positive immunomodulatory effects of BBR treatment on $CD4^+$ T cells, we performed adoptive transfer experiment in $Rag^{-/-}$ mice (**Fig 2S**). Adoptive transfer of $CD4^+$ T cells from BBR treated infected mice into $Rag^{-/-}$ mice significantly reduced bacterial burden in the lungs (**Fig 2T**) and the spleen (**Fig 2U**) of $Rag^{-/-}$ mice upon *M.tb* infection concluding that BBR exerts host-protective effects by enriching *M.tb* specific $CD4^+$ T cell responses.

BBR enriches pathways associated with establishment of T_{RM} in human PBMCs

Fig 3A represents a simplistic model of T cell differentiation into different memory subsets highlighting different regulators and surface markers used to identify these cells. To understand the molecular signaling involved in the enhancement of $CD4^+$ adaptive memory after BBR treatment, we cultured PBMCs isolated from healthy PPD^+ individuals in the presence of BBR for 48h. Intriguingly, BBR treatment drove significant differentiation of $CD4^+$ T_{NAIVE} cells into T_{EM}, T_{EMRA} and T_{RM} T cell subsets with no significant increase in T_{CM} cells (**Fig 3B–3G**). To understand the mechanistic details of heightened memory responses, we performed the whole proteome analysis of human PBMCs with or without BBR treatment. In each individual, BBR treatment induced a distinct proteome landscape with a significant number of differentially expressed proteins (**Fig 3H**). Interestingly, BBR treatment collectively downregulated the expression of 323 proteins (**Fig 3I**) and induced the expression of 527 proteins (**Fig 3J**) in the treated PBMCs. Further analysis on these commonly expressed proteins revealed few pathways which were downregulated upon BBR treatment (**Fig 3K**). Curiously, diverse pathways associated with key cellular processes such as cell cycle, cell adhesion, cell division and glycolysis were upregulated upon BBR treatment (**Fig 3L**). Importantly, BBR treatment enhanced the upregulation of critical proteins of Notch signaling pathway (**Fig 3L and 3M**) which is known to stimulate the differentiation and maintenance of T_{RM} cells [30].

TCR stimulation along with downstream signalling pathways such as PI3K/AKT/mTOR play a critical role in shaping the T cell memory [12]. While activated AKT is known to phosphorylate FOXO1 triggering its nuclear exclusion, previous literature highlights the importance of FOXO1 mediated gene expression in the generation and maintenance of protective memory cells [31,32] Further, Blimp1 transcription factor is known to regulate resident memory responses at the local site of infection [33,34]. Ironically, Notch3 transactivates PTEN which in turn inhibits the AKT signaling [35] leading to FOXO1 activation (**S7A Fig**). We validated these targets by RT-PCR and observed that BBR treatment induced significant expression of genes related to notch signaling as well as the downstream targets such as Foxo1, Pten and Blimp1 (**Fig 3N**). Moreover, BBR inhibited AKT and FOXO1 phosphorylation (**Figs 3O and 3P and S7B–S7D**) and along with AKT inhibitor (AKTi), BBR synergistically reduced T_{NAIVE} population (**S7E Fig**), increased T_{EM} (**S7F Fig**) and T_{EMRA} cells (**S7G Fig**) with no effect on T_{CM} cells (**S7H Fig**). BBR treatment also enhanced resident memory functions by modulating the BLIMP-1 expression (**Fig 3Q**).

Cellular metabolism plays a crucial role in modulating T cell effector functions [36] while BBR is known to induce glycolysis in many cell types [37,38], (**S7I Fig**). Consistent with the previous findings and our proteomics data, BBR significantly induced glycolysis (**Fig 3R**) in human PBMCs. Furthermore, to dwell deeper into the immunological milieu induced upon BBR treatment, Bio-plex Pro Human cytokine screening Panel (48-Plex) was utilised to screen the regulation of cytokines in human PBMCs. BBR treatment consistently enhanced the expression of pro-inflammatory cytokines in human PBMCs (**Fig 3S–3V**) derived from PPD^+ individuals. Moreover, 20 pro-inflammatory cytokines and chemokines were upregulated in

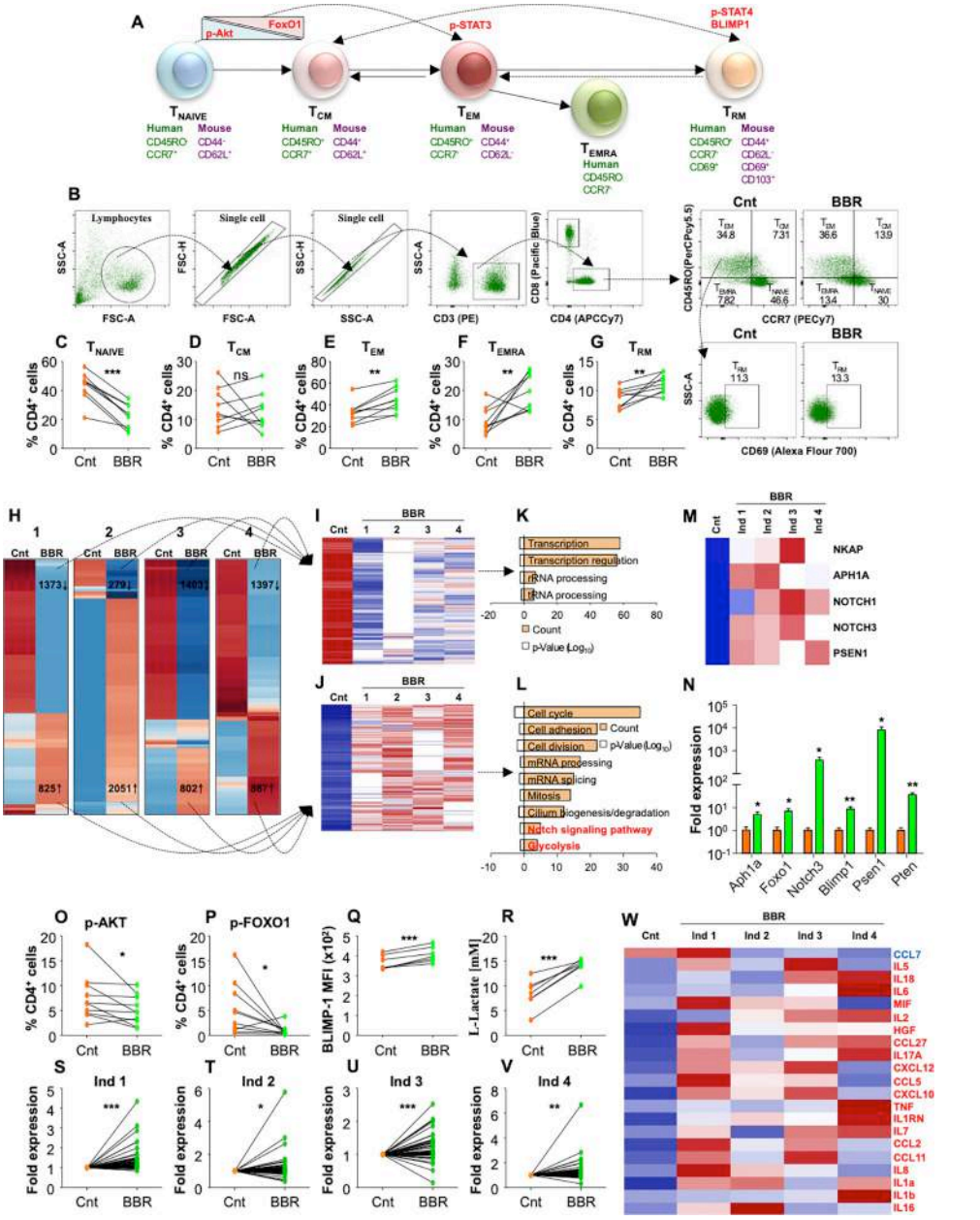

Fig 3. BBR treatment enriches human CD4$^+$ memory T cells by regulating NOTCH/PTEN/Akt/FOXO1 pathway. **(A)** Schematic representation of T cell differentiation into T_{EM}, T_{CM} and T_{RM} memory subsets. **(B-G)** Human PBMCs isolated from 7 PPD$^+$ healthy individuals were ex vivo stimulated with CSA and treated with BBR (10 μg/ml) for 48 h followed by surface staining with α-CD3 (PE), α-CD4 (APCCy7), α-CD8 (Pacific Blue), α-CD45RO (PerCPCy5.5), α-CCR7 (PECy7) and α-CD69 (Alexa Flour 700) **(B)** Gating strategy employed to depict the different memory T cell subsets. Percentage of **(C)** CD4$^+$ T_{NAIVE} cells, **(D)** CD4$^+$ T_{CM} cells, **(E)** CD4$^+$ T_{EM} cells, **(F)** CD4$^+$ T_{EMRA} cells and **(G)** CD4$^+$ T_{RM} cells. **(H)** Whole proteome profiling of untreated and BBR treated human PBMCs derived from 4 PPD$^+$ healthy individuals. Heat map representation of the differentially expressed proteins (Log2 fold, n = 3). Common proteins in all the individuals that are **(I)** downregulated and **(J)** upregulated upon BBR treatment. Biological processes that are **(K)** downregulated and **(L)** upregulated upon BBR treatment. **(M)** Notch signalling pathway associated proteins which were upregulated in human PBMCs upon BBR treatment. **(N)** RT-PCR of genes related to Notch signaling pathway. **(O)** Human CD4$^+$ T cells expressing p-AKT and **(P)** human CD4$^+$ T cells expressing p-FOXO1. **(Q)** MFI of human CD4$^+$ T cells expressing Blimp-1. **(R)** Extracellular L-Lactate quantification in untreated and BBR treated human PBMCs. **(S-W)** represents multiplex cytokines assay upon BBR treatment in human PBMCs of derived from 4 PPD$^+$ healthy individuals (refer methodology). **(S-V)** Fold expression changes of 46 cytokines upon BBR treatment in different individuals. **(W)** Heat map of common differentially expressed cytokines. In **H**, **I**, **J**, **M**, and **W**,

Red represents upregulation while blue represents downregulation. Data is representative of two independent experiments. The data values represent mean ± SD (n is 4 to 7). *p<0.05, **p<0.005, ***p<0.0005.

https://doi.org/10.1371/journal.ppat.1011165.g003

the PBMCs derived from at least 3 out of 4 individuals (Fig 3W). Overall these results indicate that BBR enhances effector functions of $CD4^+$ T cells and upregulates critical signaling associated with T_{RM} establishment and maintenance.

BBR drives the expansion of memory T cells by modulating key regulators of T cell development in murine T cells

To validate the molecular signaling involved in the enhancement of $CD4^+$ adaptive memory after BBR treatment, splenocytes isolated from *M.tb* infected mice were *ex vivo* stimulated with *M.tb* complete soluble antigen (CSA) and treated with BBR (10μg/ml) for 48h followed by immune profiling. Analysis of different $CD4^+$ T cell subsets via flow cytometry (Fig 4A) revealed that BBR treatment significantly reduced the percentage of T_{NAIVE} subset (Fig 4B) with a concomitant increase in the T_{EM} cells (Fig 4C). While no difference was observed in the T_{CM} population (Fig 4D), BBR significantly induced the T_{RM} subset (Fig 4E). Consistent with the previous results, BBR treatment significantly reduced the activation of AKT (Fig 4F and 4G) and decreased the phosphorylation of FOXO1 (Fig 4H and 4I) in $CD4^+$ T cells. Inhibition of AKT signalling has been shown to promote central memory responses by increasing nuclear accumulation of FOXO1 [39]. It is also well-established that STAT3 and STAT4 play specific function in the formation of T cell memory subsets in response to infections [16,40]. To further ascertain the influence of BBR treatment on AKT-FOXO1 axis, we repeated the *ex vivo* T cell stimulation experiment in the presence of AKTi and BBR. AKTi alone did not increase the percentage of $CD4^+$ T_{EM} and T_{RM} populations, whereas, considerable enrichment was observed upon BBR treatment alone or in combination with AKTi (Fig 4J and 4K). This infers the influence of alternate signaling pathways contributing in enhancement of memory responses upon BBR treatment. We observed that BBR treatment induced the activation of STAT3, STAT4 and BLIMP-1 in $CD4^+$ T cells (Fig 4L–4Q) which may lead to enhanced T_{RM} response. Interestingly, heightened NFκB activation was observed in BBR treated $CD4^+$ T cells (Fig 4R and 4S) leading to a significant upregulation of host protective proinflammatory responses (Fig 4T). Furthermore, BBR treatment led to enhanced glycolysis in $CD4^+$ T cells (Fig 4U). Interestingly, 2-Deoxy-D-glucose (2DG) (glycolysis inhibitor) treatment abrogated the expression of IFNγ and IL17 in BBR treated $CD4^+$ T cells (Fig 4V and 4W) indicating that BBR potentiates pro-inflammatory response through metabolic reprogramming. Overall, this concludes that BBR treatment expands memory T cell subsets with proinflammatory characteristics.

BBR induced adaptive memory enhances the BCG vaccine efficacy and reduces the rate of TB recurrence

Having established the potential of BBR to induce significant immunological memory against TB, we next investigated whether BBR co-treatment could enhance the BCG vaccine efficacy *in vivo*. C57BL/6 mice were divided in 3 groups: Cnt (un-vaccinated), BCG (BCG vaccinated) and BCG-BBR (BCG vaccinated and BBR treated), and were challenged with low dose of H37Rv through aerosol infection model (Fig 5A). 30 days after *M.tb* infection, the mice were euthanized and analysed for bacterial burden and immune profiling. Pre-challenge immune profiling of the animals revealed increased activation of $CD4^+$ and $CD8^+$ T cells in the lungs (S8A–S8E Fig) and the spleen (S8F–S8I Fig) of the BCG vaccinated and BBR treated animals

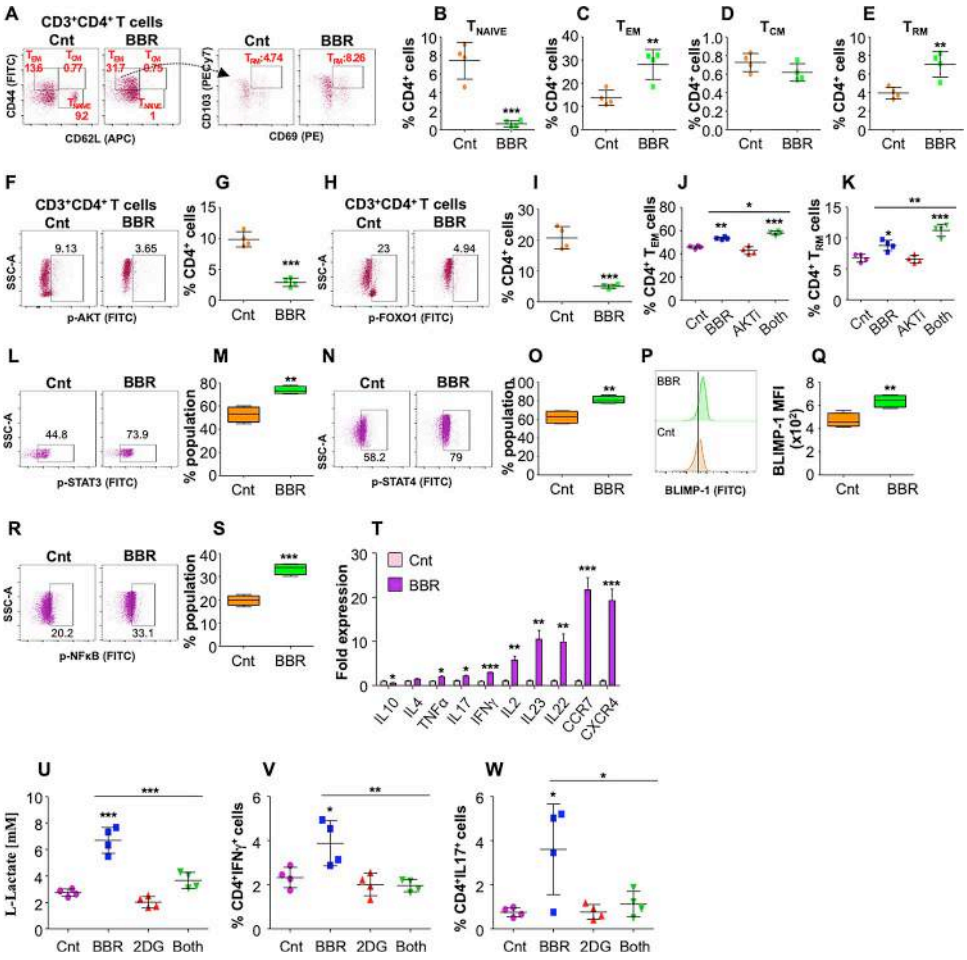

Fig 4. BBR induces expansion of antigen-specific memory T cells by targeting TCR signaling and glycolysis. Splenocytes isolated from *M.tb* infected mice were *ex vivo* stimulated with *M.tb* CSA and treated with BBR (10 μg/ml) for 48 h. *Ex vivo* stimulated splenocytes were surface stained with α-CD3 (Pacific Blue), α-CD4 (PerCPCy5.5), α-CD8 (APCCy7), α-CD69 (PE), α-CD103 (PECy7), α-CD62L (APC) and α-CD44 (FITC). **(A)** Representative dot plots and the percentage of **(B)** $CD4^+$ T_{NAIVE} cells, **(C)** $CD4^+$ T_{EM} cells, **(D)** $CD4^+$ T_{CM} cells and **(E)** $CD4^+$ T_{RM} cells after BBR treatment. **(F-I)** To analyse the activation status of key signaling molecules and transcription factors, the cells were stained with α-CD3 (Pacific Blue) and α-CD4 (PerCPCy5.5) followed by intracellular staining with antibodies against p-AKT and p-FOXO1 (see methods). **(F)** Representatives FACS scatter plots and **(G)** the percentage of $CD4^+$ T cells expressing pAKT. **(H&I)** Representative scatter plots and the percentage of $CD4^+$ T cells expressing p-FOXO1. **(J&K)** *Ex vivo* stimulated splenocytes were treated with BBR (10 μg/ml), AKTi (2.5μM) or both for 48 h followed by surface staining with α-CD3 (Pacific Blue), α-CD4 (PerCPCy5.5), α-CD69 (PE), α-CD103 (PECy7). **(J)** Percentage of $CD4^+$ T_{EM} and **(K)** $CD4^+$ T_{RM} cells. **(L-S)** Stimulation of transcription factors involved in memory responses were examined for which the cells were stained with α-CD3 (Pacific Blue) and α-CD4 (PerCPCy5.5) followed by intracellular staining with antibodies against p-STAT3, p-STAT4, BlIMP-1 and p-NFκB (see methods). Representatives FACS scatter plots and percentage of $CD4^+$ T cells expressing **(L&M)** p-STAT3, **(N&O)** p-STAT4, **(P&Q)** Blimp-1 and **(R&S)** p-NFκB. **(T)** Expression of cytokines in *M.tb* specific T cells with or without BBR treatment. **(V-X)** *Ex vivo* stimulated splenocytes isolated from *M.tb* infected mice were treated with BBR (10 μg/ml), 2-Deoxy-D-glucose (2DG; 200 mM), both or left untreated for 24 h. **(U)** L-Lactate present in the supernatant of treated splenocytes. **(V)** Percentage of $CD4^+IFN\gamma^+$ T cells and **(W)** $CD4^+IL17^+$ T cells. The data values represent mean ± SD (n = 3–4). $^*p<0.05$, $^{**}p<0.005$, $^{***}p<0.0005$.

https://doi.org/10.1371/journal.ppat.1011165.g004

as compared to the BCG vaccinated alone. Consistent with this, BBR treatment during BCG vaccination significantly decreased the bacterial burden in the lungs (Fig 5B) and the spleen (Fig 5C) of co-treated mice as compared to only BCG vaccination. Immune analysis revealed increased percentage of $CD4^+$ and $CD8^+$ T cells in the lungs (S9A–S9C Fig) as well as in the

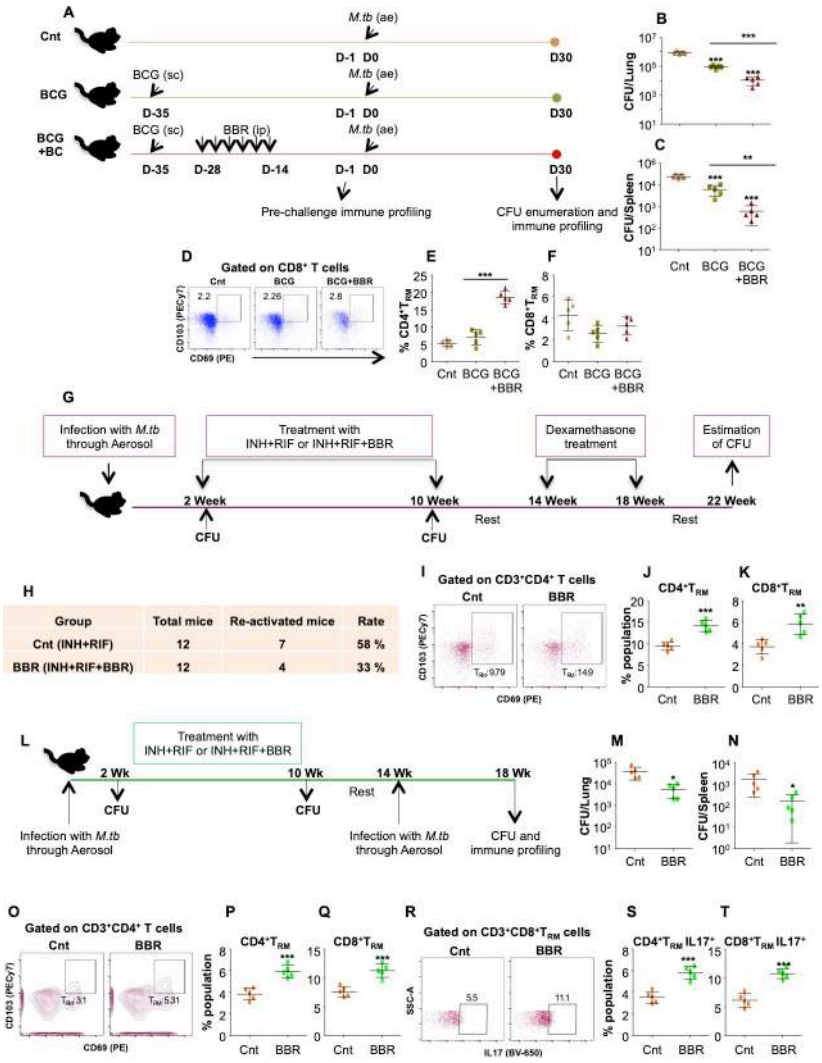

Fig 5. BBR enhances the BCG vaccine efficacy and protects against recurrent TB by inducing T cell resident memory responses in murine model. **(A)** Schematic representation of vaccine model used in the study. Bacterial load in **(B)** the lungs and **(C)** the spleen of infected mice. *Ex vivo* stimulated lung cells were surface stained with α-CD3 (Pacific Blue), α-CD4 (PerCPCy5.5), α-CD69 (PE), α-CD103 (PECy7), followed by flow cytometry. **(D)** Representative FACS plots and percentage of **(E)** $CD4^+$ T_{RM} cells and **(F)** $CD8^+$ T_{RM} cells in the lung of infected animals. **(G)** Schematic diagram representing the re-activation model used in this study. **(H)** Rate of disease relapse with and without BBR treatment. **(I)** FACS plots representing CD69 and CD103 expressing $CD4^+$ T cells and **(J)** percentage of $CD4^+$ T_{RM} cells and **(K)** $CD8^+$ T_{RM} cells in the spleen of infected mice. **(L)** Diagrammatic representation of re-infection model used in the study. Bacterial burden in **(M)** the lungs and **(N)** the spleen of re-infected mice. *Ex vivo* stimulated single cell suspensions of the lungs were stained with α-CD3 (Pacific Blue), α-CD4 (PerCPCy5.5), α-CD69 (PE), α-CD103 (PECy7), α-CD62L (APC), and α-IL17 (BV650) followed by flow cytometry. **(O)** Representative FACS plots and the percentage of **(P)** $CD4^+$ T_{RM} cells and **(Q)** $CD8^+$ T_{RM} cells in the lungs of re-infected mice. **(R-T)** Percentage of resident memory T cells producing IL17. Data is representative of two independent experiments. The data values represent mean ± SD (n = 5). $^*p<0.05$, $^{**}p<0.005$, $^{***}p<0.0005$.

https://doi.org/10.1371/journal.ppat.1011165.g005

spleen (S9D–S9F Fig) of co-vaccinated mice. BCG primarily induces effector memory responses as a result of which the anti-TB immunity induced by BCG is short lived and wanes in adults [41]. Interestingly, with no effect in the lungs (S9G–S9I Fig), BBR treatment increased the $CD4^+$ and $CD8^+$ T_{CM} cells in the infected spleen (S9J–S9L Fig). Furthermore, the percentage of T_{RM} cells was significantly high in the lungs (Fig 5E and 5F) and the spleen

(S9M–S9O Fig) of infected BCG-BBR vaccinated and treated animals as compared to the BCG vaccination alone.

Memory T cells are vital for long-term immunity against disease relapse due to re-activation or re-infection. To further provide the *in vivo* evidence of the above results, we performed reactivation study in murine model (Fig 5G). BBR co-therapy significantly reduced the rate of disease re-activation (Fig 5H) further proving that BBR treatment generates long-term *M.tb* specific protective memory responses with boosted T_{CM} (S10A–S10C Fig) and T_{RM} populations (Fig 5I–K) in the lungs of infected mice. Furthermore, in re-infection murine model of TB (Fig 5L), the bacterial burden was significantly reduced in the lungs (Fig 5M) and the spleen (Fig 5N) of re-infected mice previously treated with INH+RIF+BBR (BBR group) as compared with INH+RIF group (Cnt group). Immune profiling revealed increased percentage of T_{RM} cells in the lungs (Fig 5O–5Q) and the spleen (S10D and S10E Fig) of re-infected animals treated with INH+RIF+BBR. IL17 plays a crucial protective role in the recall protection to *M.tb* infection [6,11]. Interestingly, IL17 secreting T_{RM} population was enriched in the lungs (Fig 5R–5T) and the spleen (S10F and S10G Fig) of BBR treated mice. Similar trend was observed for the T_{CM} population in both the organs (S10H–S10Q Fig). Collectively, our preclinical mice and human data projects BBR as an excellent immunotherapeutic and immunoprophylactic candidate against susceptible and drug resistant TB.

Discussion

Immunological memory can be delineated as modification in immune responsiveness after the primary encounter to elicit prompt and robust immune responses. With more profound insights, the conventional characterization of immunological memory is continuously advancing. Since an upsurge in incidences of drug-resistant TB along with recurrence and reactivation of *M.tb* infection is the root cause of morbidity and mortality worldwide, the utmost significance of immunological memory to combat TB remains unchanged [42]. Therefore, an efficacious immunomodulatory strategy is deemed indispensable to enhance population-wide immune protection to moderate the global TB burden. Strategic host-directed therapies to augment protective immune responses, accomplish bacterial sterility, and subside detrimental pathology are endeavoured [24] to improve clinical outcomes in TB patients [43,44]. Combinatorial administration of immunotherapeutic has resolved inadequacies of numerous stratagems and was found advantageous in eliminating *M.tb* infections in several clinical trials [45]. One of the most established immunotherapeutic BBR has been known for ages for its effective therapeutic potential to treat diabetes and many other diseases [46,47]. Despite this, the prospects of BBR for better clinical recovery during *M.tb* infection by augmenting immunological memory responses have not been evaluated.

In line with the previous literature [27], in this study we demonstrated the anti-mycobacterial potential of BBR in murine macrophages, human monocytic cell line THP-1, and murine model against susceptible and drug-resistant strains of *M.tb*. Mononuclear phagocytic cells are prominent in activating T cells but during the pathogenic hijack, apoptotic inhibition occurs that restricts the presentation of bacterial antigen and further delays T cell mediated adaptive immune response [48]. We found that BBR prompted apoptotic cell death in infected macrophages which constrains *M.tb* infection. With little direct anti-mycobacterial activity, BBR greatly enhanced the host defence mechanisms by modulating NF-κB and STAT-3 signaling [49]. BBR also increased the percentage of co-stimulatory molecules on mouse peritoneal macrophages and enriched the host protective chemokines, cytokines in response to *M.tb* infection which was further trailed in line with T cell responses. BBR treatment also enhanced the killing potential of T cells as was evident by the results of *ex vivo* co-culture experiments. BBR

administration in adjunct to INH reduced the bacterial burden in human monocytic cell line THP-1 as well as peritoneal macrophages. Furthermore, BBR significantly boosted the extermination of drug-resistant MDR and XDR strains of *M.tb*.

The therapeutic effects of BBR have been evaluated for diverse diseases in murine models, with no significant toxicity [50,51]. So, comprehensive immunological analysis was performed in the murine model of TB. Recently a piecemeal study has evaluated the impact of BBR treatment in adjunct to front-line TB drugs INH and RIF against drug-susceptible *M.tb* strain [27] wherein BBR as an adjunct did not demonstrate any additive or synergistic effect on the bacterial load. In our study, we have defied numerous shortcomings of this study. First of all, our study extensively validates the effectiveness of BBR in eliciting anti-mycobacterial immune responses against drug-susceptible and resistant strains of *M.tb* exclusive of ATT drugs. We also demonstrate the effectiveness of BBR in reversing the immune dampening effects of INH. Augmented efficacy of BBR in terms of lower bacterial burden, reduced lung inflammation and heightened host protective immune response either alone or in combination with INH can be attributable to a long treatment regimen of 45 days in our study. Moreover, BBR was administered intraperitoneally for superior circulation. Treatment was scientifically strategized to downgrade hepatotoxicity and to enhance host protective responses. BBR administration significantly reduced the bacterial load in adjunct to frontline anti-TB drug INH and resultant diminution in pathological damage in the lungs as reported recently [27]. Our results also demonstrate the effectiveness of BBR treatment in significantly lowering the bacterial load in MDR and XDR infected animals. Hence, it can be stated decisively that BBR elicits anti-mycobacterial immune responses against a range of *M.tb* strains. Furthermore, with no prior information on BBR induced mechanisms of protection against TB, we have comprehensively evaluated the impact of BBR on T cell signal transduction linking it with the establishment of durable immunological memory against *M.tb*.

To decipher the immunological feature of BBR induced reduction in bacterial burden, immune profiling was performed. Activation of adaptive immune cell populations was observed in compliance with an increase in the percentage and the activation of innate immune cells upon BBR treatment. In case of inflammatory bowel disease, BBR is known to induce protective immune responses by modulating IFNγ and IL17 $CD4^+$ T cells by activation of AMP kinase [52]. IFNγ plays a vital role during *M.tb* infection by stimulating Th1 induction from naïve $CD4^+$ T cells [53] and IL17 plays a significant role by stimulating recall responses during recurrent *M.tb* infections [11,54,55]. In agreement with the previous reports, BBR treatment resulted in the increased percentage of IFNγ and IL17 secreting $CD4^+$ and $CD8^+$ T cells. Furthermore, BBR treatment enhanced expression of pro-inflammatory cytokines such as CCL2, IL12β, IL1β alone and in adjunct to INH. Furthermore, INH induced anti-inflammatory responses were countered along with BBR treatment.

Long-term memory particularly increased T_{CM} pool is vital for heightened immune responses against *M.tb* infections. Further, the T_{RM} population residing at the site of infection play a critical role in mediating diverse host protective effector functions. T_{RM} upon encountering antigen stimulates IFNγ production and recruits memory T cell and other immune cell populations to the site of infection [56,57]. Our research presents strong evidence of the augmented T_{RM} and T_{CM} responses upon BBR therapy alone and in adjunct to INH. These results were further strengthened by BCG vaccination experiments wherein we observed a striking reduction in the bacterial burden on administering BBR post BCG immunization in *M.tb* infected mice. In agreement with previous results, we observed a superior percentage of T_{CM} and T_{RM} cell responses upon BBR treatment subsequent to BCG immunization. This again highlights the prominence of this immunomodulatory strategy to provide ever-lasting immunity against *M.tb* infections. Further, the biological evidence of long-term protective immune prophylactic effects of BBR were provided by re-infection and re-activation mice experiments

wherein BBR treated animals displayed increased T_{CM} and T_{RM} cell responses leading to a significantly lower bacterial burden and reduced relapse rate.

To dwell into the immune mechanisms by which the attributes of immunological memory were enhanced upon BBR treatment, we performed *ex vivo* studies with *M.tb* specific T cells and observed that BBR treatment instigated significant differentiation of T_{NAIVE} population into T_{EM} and T_{RM} cells. It is well-established that naïve T cells, T_{CM} and T_{EM} cells are capable to differentiate into T_{RM} cells upon stimulation [58]. Previously it has been reported that the T_{RM} cells have a definite cytokine profile (TGFβ, IL15, Type I IFN, IL12) as well as T_{RM}-specific transcription factors such as Runx3, Hobit, Blimp1etc [59] that distinguish them from other immune cell populations and enriching selective and protective tissue specific immunity. Apart from this, certain studies have ascertained the critical role of STAT4 in regulating T_{RM} differentiation and persistence in achieving tissue-specific immunity against infections [40]. *Ex vivo* BBR treatment elicited the expansion of T cell memory pool by modulating vital interconnected immune molecules such as AKT, FOXO-1, STAT-3, STAT-4, BLIMP-1 as well as NFκB. Instigation of memory establishment was in agreement with the enhancement of pro-inflammatory cytokines such as IFNγ, IL2, IL23, IL22, CCR7 and CXCR4 in BBR treated *M.tb* specific T cells. Furthermore, BBR induced metabolic flux towards glycolytic pathway thereby enhancing effector functions of $CD4^+$ T cells secreting key host protective cytokines- IFNγ and IL17.

Many times, the results obtained with mice studies poorly mimic conditions of human physiology. To ascertain the memory inducing potential of BBR in humans, we performed *ex vivo* experiments with PBMCs isolated from PPD^+ healthy donors. To our satisfaction, BBR treatment resulted in a significant reduction in $CD4^+$ T_{NAIVE} population with a concomitant increase in $CD4^+$ T_{EM}, T_{EMRA} and T_{RM} subsets. Moreover, BBR treated human PBMCs also displayed reduced phosphorylation of AKT which led to an enhanced FOXO1 activation as BBR/AKTi treatment synergistically decreased $CD4^+$ T_{NAIVE} population and increased T_{EM} and T_{EMRA} subsets. Additionally, BLIMP-1, a T_{RM} specific transcription factor was also upregulated in the BBR treated PBMCs [60]. Similar to the mice *ex vivo* experiments, BBR treatment heightened glycolytic flux in human PBMCs along with boosted pro-inflammatory cytokine profile. Furthermore, whole proteome analysis revealed upregulation of vital cellular processes in BBR treated human PBMCs including maintenance of glycolysis which is necessitated for T cell effector functions [61] and Notch signaling pathway critically known for T_{RM} establishment. Receptors, NOTCH1/3 and activators APHA1/PSEN were found to be upregulated at the RNA as well as the protein levels in the BBR treated hPMBCs. Notch signaling is known to induce PTEN expression which in turn activates FOXO1 by inhibiting AKT [35,62]. Convincingly, BBR treatment significantly induced the expression of PTEN and FOXO1 in human PMBCs. Based on these results; we propose a probable mechanism of action by which BBR enhances the immunological memory against TB (**Fig 6**).

Finally, this study substantiates the prospects of BBR as a potent immunomodulator that strikingly augments protective immunological memory responses against *M.tb* infection. Further corroboration in the higher TB model that shares more similarities with humans such as non-human primates will be valuable to appraise BBR as promising host-directed therapy against susceptible and drug-resistant TB.

Methodology

Ethics statement

Animal experiments were executed as per the regulations stated by the Institutional Animal Ethics Committee of the International Centre for Genetic Engineering and Biotechnology (ICGEB, New Delhi, India) along with the Department of Biotechnology (DBT) standards

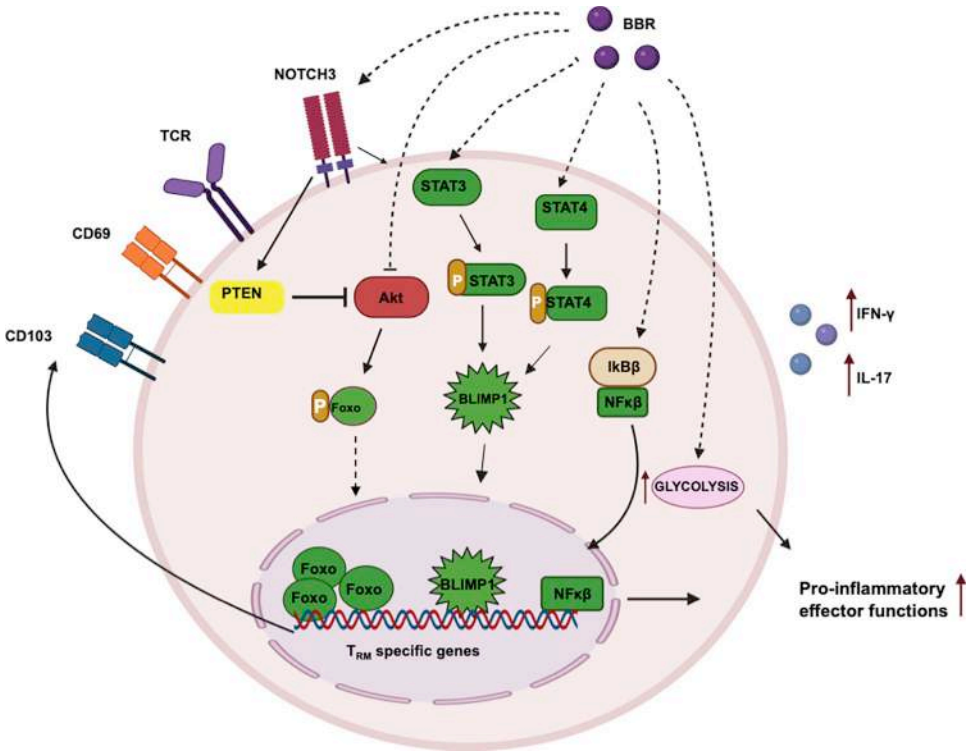

Fig 6. BBR instigates host-protective immune responses against M.tb by directing key immunological signaling pathways. In response to *M.tb* infection, BBR establishes long-lived, host protective resident memory T cells (TRM) at the site of infection. BBR enhances the effector functions of T lymphocytes by enhancing CD69 expression, directing metabolic flux towards glycolysis, activation of key host protective signaling pathways, and pro-inflammatory immune responses. BBR enriches pathways essential for the establishment and maintenance of memory T cells. BBR upregulates NOTCH3 which directs PTEN to simultaneously inhibit AKT and activate STAT signaling. AKT inhibition further decreases FOXO1 phosphorylation thereby enhancing its nuclear retention. BBR-mediated enhancement of activated STAT4 and STAT3-mediated BLIMP1 signaling axis further results in heightened expression of TRM-specific genes for long-term protection against M.tb infections.

https://doi.org/10.1371/journal.ppat.1011165.g006

(Government of India) (Approval ID: ICGEB/IAEC/08/2016/IMB-1, ICGEB/IAEC/08092021/IMB-19). All the animals utilized in the investigation were ethically sacrificed by asphyxiation with carbon dioxide adhering to institutional and DBT practices.

All the experiments related to human samples were performed as per the regulations stated by the Institutional Ethics Committee of Institute of Liver and Biliary Sciences (ILBS), New Delhi along with the Department of Biotechnology (DBT) standards (Government of India) (Approval ID:IEC/2021/70/NA6). Human samples were handled by a skilled technician, samples were coded to maintain records, and consent forms were signed by all the participants before sample acquisition.

Mice

C57BL/6 mice of 6–8 weeks were maintained in the Animal facility at ICGEB, New Delhi, India. Mice were accessed and obtained for experimental procedures from the facility.

Bacteria

The mycobacterial strains used in this study (H37Rv, Rv-GFP, MDR, and XDR) were maintained in 7H9 (Middlebrook, Difco) medium supplemented with 10% ADC (albumin,

dextrose, and catalase; Difco), 0.05% Tween 80 and 0.2% glycerol. Axenic mid-log phase cultures were cryopreserved in 20% glycerol (Sigma) and were kept at -80˚C for future purpose.

Peritoneal macrophages

Mice were intraperitoneally injected with 2ml of 4% thioglycolate broth (BD) five days prior to the experiment. Cells were isolated from the peritoneal cavity using ice-cold sterile PBS and were cultured in RPMI-1640 medium supplemented with 10% fetal bovine serum (Thermo fisher scientific Inc or Hyclone) followed by overnight incubation at 37˚C and 5% CO_2. Non-adherent cells were removed by washing with sterile PBS while adherent monolayer of cells was used for further experiments. The homogeneity of isolated macrophages was analysed by staining with CD11b antibody followed by flow cytometry.

Ex vivo infection, cell death, Apoptosis assay & CellROX assay

Peritoneal macrophages or PMA- differentiated THP1 cells were used for *ex vivo* experiments. For checking the cytotoxicity of BBR, mouse peritoneal macrophages were treated with different concentrations of BBR for 48 h followed by propidium iodide (PI) staining as described elsewhere [21]. Since 20 μg/ml of BBR was chosen for future experiments, a time dependent PI cytotoxicity assay was performed at this concentration. For infections, bacterial cryostocks were revived and single cell suspensions were formed. Macrophages were infected with *M.tb* strains at 1:10 MOI. Four hours post-infection, cells were washed twice with 1X PBS so as to remove the extracellular bacteria. Cells were treated with 20 μg/ml of BBR and then incubated at 37˚C for different time points followed by CFU enumeration [63], immunoblotting, RNA isolation or flow cytometry. Apoptosis was detected by staining the cells with Annexin V/7AAD (Biolegend) as per manufacturer's protocol. CellROX (ThermoFisher Scientific) was used to detect the intracellular ROS in the *M.tb* infected peritoneal macrophages after treatment with 20 μg/ml of BBR for 24 h [64].

Human PBMC isolation

Blood samples from 10 healthy individuals were collected in BD vacutainer blood collection tubes and were layered onto Histopaque 1077 (Sigma-Aldrich) followed by centrifugation at 400g for 30 minutes at 25˚C. The opaque interface containing PBMCs were gently transferred and suspended in complete RPMI-1640 medium. These cells were then pelleted, counted, and seeded in the 12-well plates for further experiments.

Western blot analysis

RIPA buffer (50 mM Tris, pH 8.0, 150 mM NaCl, 1.0% NP-40, 0.5% Sodium deoxycholate, 0.1% SDS) supplemented with 1X protease and phosphatase inhibitor cocktail (thermos scientific) was used to lyse the cells. Protein concentration in samples was estimated using Bradford assay. Samples were run on 10% polyacrylamide gel followed by transfer on PVDF membrane (Millipore). Membrane was then blocked with 5% BSA dissolved in PBST (PBS and 0.1% Tween-20), followed by overnight probing for diverse proteins with respective antibodies. Chemiluminescent HRP substrate (ECL, Millipore) was layered to develop blots on Image-Quant LAS 500.

qPCR analysis

Total RNA was isolated from peritoneal macrophages and splenocytes by standard RNA isolation protocol followed by cDNA synthesis using iScript cDNA synthesis kit (Bio-Rad). Real-

time PCR was performed using SYBR Green Master Mix (Bio-Rad). Bio-Rad Real-Time thermal cycler (BioRad, USA) was used for Real-time quantitative RT-PCR analysis. The list of Primers used in the study are provided in the S1 Table.

Mice infection with *M.tb* and CFU enumeration

Mice were infected with drug-susceptible and resistant strains of *M.tb* via aerosol route using Madison aerosol chamber (University of Wisconsin, Madison, WI) with its nebulizer pre-adjusted to deposit approximately 110 CFUs to the lungs of mice. Axenic cultures were sonicated to prepare 15 ml of bacterial single-cell suspension for infection. 5–6 mice from each group were euthanized at different time points to determine the bacterial burden. Lungs and spleen were isolated and homogenized in sterile PBS and were plated onto 7H11 Middlebrooks (Difco) plates containing 0.05% Tween-80, 10% oleic acid, albumin, dextrose, and catalase (OADC) (Difco). The homogenates were plated in different dilutions and were incubated at 37˚C for 21–28 days. *M.tb* colonies were counted and CFU was enumerated at various time points.

Drug administration

For *ex vivo* infection experiments, macrophages were treated with 20μg/ml of BBR (Sigma). Furthermore, immunological memory was analysed in human PBMCs and mice splenocytes utilising 10 μg/ml of BBR (Sigma). For mice studies, 4 mg/kg of BBR dissolved in 100 μl of PBS with 5% DMSO was injected intraperitoneally for 45 days thrice a week, whereas the control group received only vehicle. 100 mg/L of INH and 60 mg/L RIF were administered in drinking water which was changed every alternative day.

Adoptive cell transfer therapy

To ascertain the *M.tb* specific immune response, the harvested lungs from BBR treated group was macerated using sterile frosted slides to prepare single cell suspension. Subsequently the stained $CD4^+$ T cells were sorted and cultured overnight in complete RPMI. Approximately one million cells were injected intravenously to Rag1-/- mice and further given low dose aerosol 5 days post transfer. Lung and spleen were then isolated after 21 days to determine the bacterial load.

Multiplex cytokines immunoassay

Supernatant of 24h cultured Human PBMCs was collected and dilutions were prepared for sample and standard using Bio-Plex Pro Human Cytokines Assay Instructions manual. Detecting antibody was further added followed by Streptavidin-PE incubation. Data was acquired using Bio-Plex system and then analysed.

Mass spectroscopy

10μg of protein was isolated from Control and BBR treated Human PBMCs and then desalted by reduction, alkylation and digestion using Trypsin Gold, Mass Spectrometry Grade (Promega Corporation, WA, USA) for 24hrs at 37˚C for LC-MS/MS analysis. The peptides formed were extracted on a 25-cm analytical C18 column (C18, 3 μm, 100 Å), by (5–95%) gradient of buffer B (aqueous 80% acetonitrile and 0.1% formic acid) at a flow rate of 300 nL/min for 2.5 hrs. Subsequently, these peptides were exposed to nano-electrospray ionisation and Tandem mass spectrometry (MS/MS) by the application of Q-Exactive (Thermo Fisher Scientific, San Jose, CA, United States) at the collision-induced dissociation mode with the electrospray

voltage of 2.3 kV. Data analysis comprising of standard statistical analysis, network and pathway analysis was done by Proteome Discoverer (version 2.0, Thermo Fisher Scientific, Waltham, MA, United States).

BCG vaccination

Mice were vaccinated subcutaneously with the single dosage of 1×10^6 colony forming units (CFUs) of BCG Pasteur strain in 100 μL of sterile saline. Subsequent to 7 days rest post-vaccination, the mice were treated with 4 mg/kg of BBR, thrice a week for 14 days intraperitoneally. After 14 days of break, the mice were then challenged via aerosol infection of *M.tb* strain H37Rv. Organs were harvested to elucidate bacterial burden and immune profiling within 30 days post-infection.

Reinfection and Reactivation experiments

To undermine the susceptibility of *M.tb* infection, studies were performed in reactivation and reinfection models. Low dose aerosol of H37Rv was given to the mice and treated with INH (100 mg/L) and RIF (40 mg/kg) in drinking water for 12 weeks and rested for 30 days. Thereafter, the group was again challenged with *M.tb* infection followed by immune response and bacterial load determination. For reactivation studies, the mice were given dexamethasone (5 mg/kg) intraperitoneally, thrice a week for 30 days and so enumerated CFU and host protective immunological profiles.

L-Lactate quantification

Extracellular L-Lactate levels were measured in the culture supernatant from splenocytes treated with BBR and 2DG. The experiment was performed using L- Lactate assay kit (Cayman Chemicals) as per the manufacturer's guidelines.

Flow cytometry

Lungs and spleen from mice of different groups were isolated and macerated using frosted slides in ice-cold RPMI 1640 (Hyclone) supplemented with 10% FBS to prepare single-cell suspension. RBC lysis buffer was used to lyse RBCs and cells were washed with 10% RPMI 1640. After cell counting, 1×10^6 cells were seeded in 12 well for staining. For surface staining, cells were activated by 10 μg/mL of H37Rv complete soluble antigen (CSA) stimulation. Subsequently, 0.5 μg/mL Brefeldin A and 0.5 μg/mL of Monensin solution (BioLegend) were added during the last 4 hours of culture. Cells were then washed twice with FACS buffer (PBS + 3% FBS) and stained with antibodies directed against surface markers followed by fixation with 100 μl fixation buffer (biolegend) for 30 min. For intracellular staining, the cells were permeabilized using 1X permeabilizing buffer (Biolegend) and then were stained with fluorescently labelled anti-cytokine antibodies. For non-flurochrome tagged antibodies, secondary antibody tagged with Alexa Fluor 488 was used to measure the flurochrome intensity. The intensity of fluorochromes were assessed by flow cytometry (BD LSRFortessa Cell Analyzer—Flow Cytometers, BD Biosciences) followed by data analysis via FlowJo (Tree Star, USA).

Antibodies

Following antibodies were used for this study:

Anti-Mouse: CD3-Pacific Blue, CD4-PerCPCy5.5, CD8-APCCy7, CD69-PE, CD44-FITC, CD62L-APC, CD103-PeCy7, CD69-FITC, IFNγ-APC, IFNγ-BV510, IL17-PECy7,

IL17-BV650, CD11b-APCCy7, CD11c-APC, CD80-FITC, CD86-PerCPCy5.5, CD40-PE, CD4-PE, CD4-APC and CD4-FITC, CD3-BV510, CD3-BV650 from Biolegend, USA.

Anti-human: CD3-PE, CD4-APCCy7, CD8-Pacific Blue, CD45RO (PerCPCY5.5), CCR7 (PeCy7), CD69 (Alexa Fluor 700) from BD Biosciences.

Anti-human/anti-mouse: STAT3, p-STAT3, STAT4, p-STAT4, AKT, p-AKT, FOXO1, p-FOXO1, NFκB, p-NFκB, BLIMP1 and β-Tubulin from Cell Signaling Technology.

Histopathology

Lungs harvested from infected animals were fixed with 10% neutral buffered formalin, and H&E staining was performed on 5-μm-thick paraffin-embedded tissues and were examined under microscope. Granulomas for each animal in every group were screened in 5 different fields. Submitted images are representative of all the visualized section images.

Statistical analysis

All the experimental data was analysed using GraphPad Prism Software. Significant differences between the groups were determined by 2 tailed unpaired Student's t-test or 1-way ANOVA. Human data was analysed by 2 tailed paired Student's t-test. $^{*}p < 0.05$, $^{**}p < 0.005$, $^{***}p < 0.0005$.

Supporting information

S1 Fig. BBR possess weak anti-mycobacterial activity. Exponential cultures of *M.tb* strains H37Rv, MDR (Jal 2261) and XDR (MYC 431) were treated with different concentrations of BBR. OD_{600} of **(A)** H37Rv, **(B)** MDR, and **(C)** XDR cultures at day 0, day 2 and day 5 post treatment with BBR. **(D)** Cytotoxicity of BBR (different concentrations) on mouse peritoneal macrophages determined by PI staining at 48h post treatment. **(E)** Time kinetics of cytotoxicity of BBR (20 μg/ml) on mouse peritoneal macrophages determined by PI staining. **(F)** Representative histograms and **(G)** quantification of cellular ROS in *M.tb* infected macrophages with and without BBR treatment. **(H)** Percentage of apoptotic cells in uninfected macrophages 48h after treatment with BBR (20μg/ml). **(I)** OD_{600} of H37Rv cultures treated with BBR (20μg/ml) or INH (1μg/ml) or both for 5 days. Data is representative of at least two independent experiments. The data values represent mean ± SD (n = 3 to 4). $^{*}p<0.05$, $^{**}p<0.005$, $^{***}p<0.0005$.
(TIFF)

S2 Fig. BBR activates innate immune cells in the lungs and the spleen of infected mice. **(A-H)** Single cell suspensions generated from the infected lungs and spleen were *ex vivo* stimulated with *M.tb* complete soluble antigen (CSA) for 16 h followed by surface staining with antibodies against CD11b (APCCy7), CD11c (APC), CD80 (FITC) and CD86 (PerCPCy5.5) and subjected to flow cytometry. **(A)** Representative contour plots and the percentage of **(B)** $CD11b^+$ and **(C)** $CD11c^+$ cells in the infected lungs. **(D)** Representative dot plots and the percentage of **(E)** $CD11b^+CD80^+$, **(F)** $CD11b^+CD86^+$, **(G)** $CD11c^+CD80^+$ and **(H)** $CD11c^+CD86^+$ cells in the lungs of infected animals. **(I)** Representative dot plots depicting the percentage of **(J)** $CD11b^+$ and **(K)** $CD11c^+$ cells in the infected spleen. **(L)** Representative dot plots and the percentage of **(M)** $CD11b^+CD80^+$, **(N)** $CD11b^+CD86^+$, **(O)** $CD11c^+CD80^+$, and **(P)** $CD11c^+CD86^+$ in the infected spleen. Data is representative of two independent experiments. The data values represent mean ± SD (n = 5). $^{*}p<0.05$, $^{**}p<0.005$, $^{***}p<0.0005$.
(TIFF)

S3 Fig. BBR induces the activation of Th1/ Th17 immune responses in the spleen of infected mice. **(A-E)** *Ex vivo* stimulated splenocytes were surface stained with α-CD3 (Pacific Blue), α-CD4 (PerCPCy5.5), α-CD8 (APCCy7) and α-CD69 (FITC) followed by flow cytometry. **(A)** FACS dot plots and the percentage of **(B)** $CD4^+$, **(C)** $CD4^+CD69^+$, **(D)** $CD8^+$ and **(E)** $CD8^+CD69^+$ T cells in the spleen of infected mice. **(F-J)** *Ex vivo* stimulated splenocytes treated with monensin and brefeldin A for 2h and surface stained with α-CD3 (Pacific Blue), α-CD4 (PerCPCy5.5) and α-CD8 (APCCy7) followed by intracellular staining with α-IFNγ (APC) and α-IL17 (PECy7). **(F)** Representative dot plots and the percentage of **(G)** $CD4^+IFN\gamma^+$, **(H)** $CD4^+IL17^+$, **(I)** $CD8^+INF\gamma^+$ and **(J)** $CD8^+IL17^+$ cells in the infected spleen. Data is representative of two independent experiments. The data values represent mean ± SD (n = 5). $^*p<0.05$, $^{**}p<0.005$, $^{***}p<0.0005$.
(TIFF)

S4 Fig. Memory T cell responses in the spleen of infected mice. *Ex vivo* stimulated splenocytes were surface stained with α-CD3 (Pacific Blue), α-CD4 (PerCPCy5.5), α-CD8 (APCCy7), α-CD62L (APC) and α-CD44 (FITC) followed by flow cytometry. **(A)** Representative dot plots and the percentage **of (B)** $CD4^+$ T_{CM} cells and **(C)** $CD8^+$ T_{CM} cells in the infected spleen. **(D-F)** T^{RM} cells were analysed by staining the splenocytes with α-CD3 (Pacific Blue), α-CD4 (PerCPCy5.5), α-CD8 (APCCy7), α-CD69 (FITC) and α-CD103 (APC) followed by flow cytometry. **(D)** Representative scatter dot-plot images and the percentage of **(E)** $CD4^+$ T_{RM} cells and **(F)** $CD8^+$ T_{RM} cells in the spleen of infected mice. Data is representative of two independent experiments. The data values represent mean ± SD (n = 5). $^*p<0.05$, $^{**}p<0.005$, $^{***}p<0.0005$.
(TIFF)

S5 Fig. BBR induces adaptive immune responses against drug-resistant TB. (A-H) *Ex vivo* stimulated lung cells isolated from the mice infected with MDR and XDR *M.tb* were surface stained with antibodies against CD3 (Pacific Blue), CD4 (PerCPCy5.5), CD8 (APCCy7) and CD69 (FITC) followed by flow cytometry. Percentage of $CD4^+$, $CD4^+CD69^+$, $CD8^+$, $CD8^+CD69^+$ T cells in the lungs of mice infected with **(A-D)** MDR TB and **(E-H)** XDR TB. **(I-P)** Stimulated lung cells were treated with monensin and brefeldin A followed by surface staining with α-CD3 (Pacific Blue), α-CD4 (PerCPCy5.5) and α-CD8 (APCCy7) and intracellular staining with α-IFNγ (APC) and α-IL17 (PECy7). Percentage of $CD4^+INF\gamma^+$, $CD4^+IL17^+$, $CD8^+IFN\gamma^+$, $CD8^+IL17$+ T cells in the lungs of mice infected with **(I-L)** MDR and **(M-P)** XDR strains of *M.tb*. Data is representative of two independent experiments. The data values represent mean ± SD (n = 5). $^*p<0.05$, $^{**}p<0.005$, $^{***}p<0.0005$.
(TIFF)

S6 Fig. BBR activates Th1/Th17 immune responses in the spleen of mice infected with MDR/XDR TB. *Ex vivo* stimulated splenocytes isolated from MDR and XDR infected mice were analysed for T cell responses as described earlier. Percentage of $CD4^+$, $CD4^+CD69^+$, $CD8^+$ and $CD8^+CD69^+$ T cells in the spleen of mice infected with **(A-D)** MDR and **(E-H)** XDR strains of *M.tb*. Percentage of $CD4^+INF\gamma^+$, $CD4^+IL17^+$, $CD8^+IFN\gamma^+$ and $CD8^+IL17^+$ T cells in the spleen of mice infected with **(I-L)** MDR and **(M-P)** XDR strains of *M.tb*. Data is representative of two independent experiments. The data values represent mean ± SD (n = 5). $^*p<0.05$, $^{**}p<0.005$, $^{***}p<0.0005$.
(TIFF)

S7 Fig. BBR induces T cell memory by modulating AKT-FOXO1 signaling in human $CD4^+$ T cells. (A) Flowchart depicting the critical components involved in the transcription of T cell resident memory-specific genes. FACS plots from a single donor representing the percentage

of $CD4^+$ T cells expressing **(B)** p-AKT and **(C)** p-FOXO1. **(D)** Representative FACS scatter plots and the percentage of **(E)** $CD4^+$ T_{NAIVE} cells, **(F)** $CD4^+$ T_{EM} cells, **(G)** $CD4^+$ T_{EMRA} cells and **(H)** $CD4^+$ T_{CM} cells in the human PBMCs treated with BBR and AKTi. **(I)** Proposed model of enhanced T cell effector functions upon BBR treatment. The data values represent mean ± SD (n is 7). $^*p<0.05$, $^{**}p<0.005$, $^{***}p<0.0005$.
(TIFF)

S8 Fig. Pre-challenge immune status of vaccinated animals. The lungs and the spleen of control, BCG and BCG-BBR vaccinated animals were harvested and analysed for T cell activation as described before. **(A)** Representative FACS plots and scatter plots depicting the percentage of $CD4^+$, $CD4^+CD69^+$, $CD8^+$ and $CD8^+CD69^+$ T cells in **(B-E)** the lungs and **(F-I)** the spleen of vaccinated animals before *M.tb* challenge. Data is representative of two independent experiments. The data values represent mean ± SD (n = 4). $^*p<0.05$, $^{**}p<0.005$, $^{***}p<0.0005$.
(TIFF)

S9 Fig. BBR elevates BCG induced adaptive memory responses in the lungs and the spleen of infected mice. Percentage of $CD4^+$ and $CD8^+$ T cells in **(A-C)** the lungs and **(D-F)** the spleen of infected animals. Percentage of $CD4^+$ T_{CM} cells and $CD8^+$ T_{CM} cells in **(G-I)** the lungs and **(J-L)** the spleen of infected animals. **(M)** FACS plots and quantification of **(N)** $CD4^+$ T_{RM} cells and **(O)** $CD8^+$ T_{RM} cells in the spleen of infected animals. Data is representative of two independent experiments. The data values represent mean ± SD (n = 5). $^*p<0.05$, $^{**}p<0.005$, $^{***}p<0.0005$.
(TIFF)

S10 Fig. Berberine counteracts recurrent TB by inducing IL17 producing memory T cells. **(A)** FACS plots representing the percentage of **(B)** $CD4^+$ T_{CM} cells and **(C)** $CD8^+$ T_{CM} cells in the lungs of re-activation group mice. Percentage of **(D)** $CD4^+$ T_{RM} cells, **(E)** $CD8^+$ T_{RM} cells, **(F)** $CD4^+IL17^+$ T_{RM} cells and **(G)** $CD8^+IL17^+$ T_{RM} cells in the spleen of re-infected mice. **(H)** FACS plots representation and the percentage of $CD4^+$ T_{CM} cells and $CD8^+$ T^{CM} cells in **(I&J)** the spleen and **(K&L)** the lungs of re-infected mice. **(M-Q)** Percentage of central memory T cells producing IL17. **(M)** Representative FACS scatter plots of and the percentage of$CD4^+IL17^+$ T_{CM} cells and$CD8^+IL17^+$ T_{CM} cells in **(N&O)** the spleen and **(P&Q)** the lungs of re-infected mice. Data is representative of two independent experiments. The data values represent mean ± SD (n is 5). $^*p<0.05$, $^{**}p<0.005$, $^{***}p<0.0005$.
(TIFF)

S1 Table. List of the Primers used in the study.
(DOCX)

Acknowledgments

We acknowledge the support of the DBT-supported Tuberculosis Aerosol Challenge Facility (TACF) and Bioexperimentation Facility at the International Centre for Genetic Engineering and Biotechnology (ICGEB), New Delhi, India, and their staff in accomplishing this work. We would like to thank Dr P Nagraja, National Institute of Immunology, New Delhi, India for providing Rag^{-1-} knockout mice.

Author Contributions

Conceptualization: Ved Prakash Dwivedi.

Data curation: Isha Pahuja, Kriti Negi, Anjna Kumari, Meetu Agarwal, Suparba Mukhopadhyay, Babu Mathew, Shivam Chaturvedi, Jaswinder Singh Maras, Ashima Bhaskar, Ved Prakash Dwivedi.

Formal analysis: Isha Pahuja, Kriti Negi, Anjna Kumari, Meetu Agarwal, Suparba Mukhopadhyay, Babu Mathew, Shivam Chaturvedi, Jaswinder Singh Maras, Ashima Bhaskar, Ved Prakash Dwivedi.

Funding acquisition: Ved Prakash Dwivedi.

Investigation: Isha Pahuja, Kriti Negi, Anjna Kumari, Meetu Agarwal, Jaswinder Singh Maras, Ashima Bhaskar, Ved Prakash Dwivedi.

Methodology: Isha Pahuja, Kriti Negi, Anjna Kumari, Suparba Mukhopadhyay, Babu Mathew, Shivam Chaturvedi, Ashima Bhaskar, Ved Prakash Dwivedi.

Supervision: Ashima Bhaskar, Ved Prakash Dwivedi.

Validation: Isha Pahuja, Kriti Negi, Ashima Bhaskar, Ved Prakash Dwivedi.

Visualization: Ashima Bhaskar, Ved Prakash Dwivedi.

Writing – original draft: Isha Pahuja, Kriti Negi, Ashima Bhaskar, Ved Prakash Dwivedi.

Writing – review & editing: Ashima Bhaskar, Ved Prakash Dwivedi.

References

1. World Health Organization. Global tuberculosis report 2021. Geneva: World Health Organization; 2021. Available: https://apps.who.int/iris/handle/10665/346387
2. Tousif S, Singh DK, Ahmad S, Moodley P, Bhattacharyya M, Van Kaer L, et al. Isoniazid Induces Apoptosis Of Activated CD4+ T Cells. J Biol Chem. 2014; 289: 30190–30195. https://doi.org/10.1074/jbc.C114.598946 PMID: 25202011
3. Negi K, Bhaskar A, Dwivedi VP. Progressive Host-Directed Strategies to Potentiate BCG Vaccination Against Tuberculosis. Front Immunol. 2022; 13: 944183. https://doi.org/10.3389/fimmu.2022.944183 PMID: 35967410
4. Flynn JL, Chan J. Immunology of tuberculosis. Annu Rev Immunol. 2001; 19: 93–129. https://doi.org/10.1146/annurev.immunol.19.1.93 PMID: 11244032
5. Choi H-G, Kwon KW, Choi S, Back YW, Park H-S, Kang SM, et al. Antigen-Specific IFN-γ/IL-17-Co-Producing CD4+ T-Cells Are the Determinants for Protective Efficacy of Tuberculosis Subunit Vaccine. Vaccines. 2020; 8: 300. https://doi.org/10.3390/vaccines8020300 PMID: 32545304
6. Khader SA, Bell GK, Pearl JE, Fountain JJ, Rangel-Moreno J, Cilley GE, et al. IL-23 and IL-17 in the establishment of protective pulmonary CD4+ T cell responses after vaccination and during Mycobacterium tuberculosis challenge. Nat Immunol. 2007; 8: 369–377. https://doi.org/10.1038/ni1449 PMID: 17351619
7. Cadena AM, Flynn JL, Fortune SM. The Importance of First Impressions: Early Events in Mycobacterium tuberculosis Infection Influence Outcome. mBio. 2016; 7: e00342–00316. https://doi.org/10.1128/mBio.00342-16 PMID: 27048801
8. Stringari LL, Covre LP, Silva FDC da, Oliveira VL de, Campana MC, Hadad DJ, et al. Increase of CD4+CD25highFoxP3+ cells impairs in vitro human microbicidal activity against Mycobacterium tuberculosis during latent and acute pulmonary tuberculosis. PLoS Negl Trop Dis. 2021; 15: e0009605. https://doi.org/10.1371/journal.pntd.0009605 PMID: 34324509
9. Shafiani S, Tucker-Heard G, Kariyone A, Takatsu K, Urdahl KB. Pathogen-specific regulatory T cells delay the arrival of effector T cells in the lung during early tuberculosis. J Exp Med. 2010; 207: 1409–1420. https://doi.org/10.1084/jem.20091885 PMID: 20547826
10. Scott-Browne JP, Shafiani S, Tucker-Heard G, Ishida-Tsubota K, Fontenot JD, Rudensky AY, et al. Expansion and function of Foxp3-expressing T regulatory cells during tuberculosis. J Exp Med. 2007; 204: 2159–2169. https://doi.org/10.1084/jem.20062105 PMID: 17709423
11. Chatterjee S, Dwivedi VP, Singh Y, Siddiqui I, Sharma P, Van Kaer L, et al. Early secreted antigen ESAT-6 of Mycobacterium tuberculosis promotes protective T helper 17 cell responses in a toll-like

receptor-2-dependent manner. PLoS Pathog. 2011; 7: e1002378. https://doi.org/10.1371/journal.ppat.1002378 PMID: 22102818

12. Daniels MA, Teixeiro E. TCR Signaling in T Cell Memory. Front Immunol. 2015; 6: 617. https://doi.org/10.3389/fimmu.2015.00617 PMID: 26697013
13. Kim EH, Sullivan JA, Plisch EH, Tejera MM, Jatzek A, Choi KY, et al. Signal integration by Akt regulates CD8 T cell effector and memory differentiation. J Immunol Baltim Md 1950. 2012; 188: 4305–4314. https://doi.org/10.4049/jimmunol.1103568 PMID: 22467649
14. Calnan DR, Brunet A. The FoxO code. Oncogene. 2008; 27: 2276–2288. https://doi.org/10.1038/onc.2008.21 PMID: 18391970
15. Rao RR, Li Q, Gubbels Bupp MR, Shrikant PA. Transcription factor Foxo1 represses T-bet-mediated effector functions and promotes memory CD8(+) T cell differentiation. Immunity. 2012; 36: 374–387. https://doi.org/10.1016/j.immuni.2012.01.015 PMID: 22425248
16. Siegel AM, Heimall J, Freeman AF, Hsu AP, Brittain E, Brenchley JM, et al. A critical role for STAT3 transcription factor signaling in the development and maintenance of human T cell memory. Immunity. 2011; 35: 806–818. https://doi.org/10.1016/j.immuni.2011.09.016 PMID: 22118528
17. Lanzavecchia A. Lack of fair play in the T cell response. Nat Immunol. 2002; 3: 9–10. https://doi.org/10.1038/ni0102-9 PMID: 11753400
18. Sallusto F, Geginat J, Lanzavecchia A. Central memory and effector memory T cell subsets: function, generation, and maintenance. Annu Rev Immunol. 2004; 22: 745–763. https://doi.org/10.1146/annurev.immunol.22.012703.104702 PMID: 15032595
19. Lanzavecchia A, Sallusto F. Progressive differentiation and selection of the fittest in the immune response. Nat Rev Immunol. 2002; 2: 982–987. https://doi.org/10.1038/nri959 PMID: 12461571
20. Henao-Tamayo MI, Ordway DJ, Irwin SM, Shang S, Shanley C, Orme IM. Phenotypic definition of effector and memory T-lymphocyte subsets in mice chronically infected with Mycobacterium tuberculosis. Clin Vaccine Immunol CVI. 2010; 17: 618–625. https://doi.org/10.1128/CVI.00368-09 PMID: 20107011
21. Bhaskar A, Kumari A, Singh M, Kumar S, Kumar S, Dabla A, et al. [6]-Gingerol exhibits potent anti-mycobacterial and immunomodulatory activity against tuberculosis. Int Immunopharmacol. 2020; 87: 106809. https://doi.org/10.1016/j.intimp.2020.106809 PMID: 32693356
22. Kumar S, Sharma C, Kaushik SR, Kulshreshtha A, Chaturvedi S, Nanda RK, et al. The phytochemical bergenin as an adjunct immunotherapy for tuberculosis in mice. J Biol Chem. 2019; 294: 8555–8563. https://doi.org/10.1074/jbc.RA119.008005 PMID: 30975902
23. Dwivedi VP, Bhattacharya D, Yadav V, Singh DK, Kumar S, Singh M, et al. The Phytochemical Bergenin Enhances T Helper 1 Responses and Anti-Mycobacterial Immunity by Activating the MAP Kinase Pathway in Macrophages. Front Cell Infect Microbiol. 2017; 7: 149. https://doi.org/10.3389/fcimb.2017.00149 PMID: 28507951
24. Germoush MO, Mahmoud AM. Berberine mitigates cyclophosphamide-induced hepatotoxicity by modulating antioxidant status and inflammatory cytokines. J Cancer Res Clin Oncol. 2014; 140: 1103–1109. https://doi.org/10.1007/s00432-014-1665-8 PMID: 24744190
25. Mahmoud A, Germoush M, Soliman A. Berberine Attenuates Isoniazid-Induced Hepatotoxicity by Modulating Peroxisome Proliferator-Activated Receptor?, Oxidative Stress and Inflammation. Int J Pharmacol. 2014; 10: 451–460. https://doi.org/10.3923/ijp.2014.451.460
26. Liang R, Yong X, Duan Y, Tan Y, Zeng P, Zhou Z, et al. Potent in vitro synergism of fusidic acid (FA) and berberine chloride (BBR) against clinical isolates of methicillin-resistant Staphylococcus aureus (MRSA). World J Microbiol Biotechnol. 2014; 30: 2861–2869. https://doi.org/10.1007/s11274-014-1712-2 PMID: 25108628
27. Ozturk M, Chia JE, Hazra R, Saqib M, Maine RA, Guler R, et al. Evaluation of Berberine as an Adjunct to TB Treatment. Front Immunol. 2021; 12: 656419. https://doi.org/10.3389/fimmu.2021.656419 PMID: 34745081
28. Peng L, Kang S, Yin Z, Jia R, Song X, Li L, et al. Antibacterial activity and mechanism of berberine against Streptococcus agalactiae. Int J Clin Exp Pathol. 2015; 8: 5217–5223. PMID: 26191220
29. Su F, Wang J. Berberine inhibits the MexXY-OprM efflux pump to reverse imipenem resistance in a clinical carbapenem-resistant Pseudomonas aeruginosa isolate in a planktonic state. Exp Ther Med. 2017 [cited 23 Jan 2022]. https://doi.org/10.3892/etm.2017.5431 PMID: 29387199
30. Wijeyesinghe S, Masopust D. Resident memory T cells are a Notch above the rest. Nat Immunol. 2016; 17: 1337–1338. https://doi.org/10.1038/ni.3617 PMID: 27849200
31. Tejera MM, Kim EH, Sullivan JA, Plisch EH, Suresh M. FoxO1 controls effector-to-memory transition and maintenance of functional CD8 T cell memory. J Immunol Baltim Md 1950. 2013; 191: 187–199. https://doi.org/10.4049/jimmunol.1300331 PMID: 23733882

32. Delpoux A, Michelini RH, Verma S, Lai C-Y, Omilusik KD, Utzschneider DT, et al. Continuous activity of Foxo1 is required to prevent anergy and maintain the memory state of CD8+ T cells. J Exp Med. 2018; 215: 575–594. https://doi.org/10.1084/jem.20170697 PMID: 29282254

33. Behr FM, Kragten NAM, Wesselink TH, Nota B, van Lier RAW, Amsen D, et al. Blimp-1 Rather Than Hobit Drives the Formation of Tissue-Resident Memory CD8+ T Cells in the Lungs. Front Immunol. 2019; 10: 400. https://doi.org/10.3389/fimmu.2019.00400 PMID: 30899267

34. Bergsbaken T, Bevan MJ, Fink PJ. Local Inflammatory Cues Regulate Differentiation and Persistence of CD8+ Tissue-Resident Memory T Cells. Cell Rep. 2017; 19: 114–124. https://doi.org/10.1016/j.celrep.2017.03.031 PMID: 28380351

35. Zhang Y-Q, Liang Y-K, Wu Y, Chen M, Chen W-L, Li R-H, et al. Notch3 inhibits cell proliferation and tumorigenesis and predicts better prognosis in breast cancer through transactivating PTEN. Cell Death Dis. 2021; 12: 502. https://doi.org/10.1038/s41419-021-03735-3 PMID: 34006834

36. Shyer JA, Flavell RA, Bailis W. Metabolic signaling in T cells. Cell Res. 2020; 30: 649–659. https://doi.org/10.1038/s41422-020-0379-5 PMID: 32709897

37. Yin J, Gao Z, Liu D, Liu Z, Ye J. Berberine improves glucose metabolism through induction of glycolysis. Am J Physiol Endocrinol Metab. 2008; 294: E148–156. https://doi.org/10.1152/ajpendo.00211.2007 PMID: 17971514

38. Li M, Zhang H, Zhang Y, Fan J, Zhu J, Gu X, et al. Berberine Modulates Macrophage Activation by Inducing Glycolysis. J Immunol Baltim Md 1950. 2022; 208: 2309–2318. https://doi.org/10.4049/jimmunol.2100716 PMID: 35428692

39. Klebanoff CA, Crompton JG, Leonardi AJ, Yamamoto TN, Chandran SS, Eil RL, et al. Inhibition of AKT signaling uncouples T cell differentiation from expansion for receptor-engineered adoptive immunotherapy. JCI Insight. 2017; 2: 95103. https://doi.org/10.1172/jci.insight.95103 PMID: 29212954

40. Bergsbaken T, Fung H, Wilson N, Teryek M. STAT4 programs CD103− tissue-resident memory cells during infection. J Immunol. 2019; 202: 189.8–189.8.

41. Moliva JI, Turner J, Torrelles JB. Immune Responses to Bacillus Calmette-Guérin Vaccination: Why Do They Fail to Protect against Mycobacterium tuberculosis? Front Immunol. 2017; 8: 407. https://doi.org/10.3389/fimmu.2017.00407 PMID: 28424703

42. Andersen P. TB vaccines: progress and problems. Trends Immunol. 2001; 22: 160–168. https://doi.org/10.1016/s1471-4906(01)01865-8 PMID: 11286732

43. Kolloli A, Subbian S. Host-Directed Therapeutic Strategies for Tuberculosis. Front Med. 2017; 4: 171. https://doi.org/10.3389/fmed.2017.00171 PMID: 29094039

44. Kumar S, Sharma C, Kaushik SR, Kulshreshtha A, Chaturvedi S, Nanda RK, et al. The phytochemical bergenin as an adjunct immunotherapy for tuberculosis in mice. J Biol Chem. 2019; 294: 8555–8563. https://doi.org/10.1074/jbc.RA119.008005 PMID: 30975902

45. Fatima S, Kumari A, Dwivedi VP. Advances in adjunct therapy against tuberculosis: Deciphering the emerging role of phytochemicals. MedComm. n/a. https://doi.org/10.1002/mco2.82 PMID: 34977867

46. Yin J, Xing H, Ye J. Efficacy of berberine in patients with type 2 diabetes mellitus. Metabolism. 2008; 57: 712–717. https://doi.org/10.1016/j.metabol.2008.01.013 PMID: 18442638

47. Imanshahidi M, Hosseinzadeh H. Pharmacological and therapeutic effects of Berberis vulgaris and its active constituent, berberine. Phytother Res. 2008; 22: 999–1012. https://doi.org/10.1002/ptr.2399 PMID: 18618524

48. Urdahl KB, Shafiani S, Ernst JD. Initiation and regulation of T-cell responses in tuberculosis. Mucosal Immunol. 2011; 4: 288–293. https://doi.org/10.1038/mi.2011.10 PMID: 21451503

49. Yan K, Da T-T, Bian Z-H, He Y, Liu M-C, Liu Q-Z, et al. Multi-omics analysis identifies FoxO1 as a regulator of macrophage function through metabolic reprogramming. Cell Death Dis. 2020; 11: 800. https://doi.org/10.1038/s41419-020-02982-0 PMID: 32973162

50. Zhou X-Q, Zeng X-N, Kong H, Sun X-L. Neuroprotective effects of berberine on stroke models in vitro and in vivo. Neurosci Lett. 2008; 447: 31–36. https://doi.org/10.1016/j.neulet.2008.09.064 PMID: 18838103

51. Lee S, Lim H-J, Park H-Y, Lee K-S, Park J-H, Jang Y. Berberine inhibits rat vascular smooth muscle cell proliferation and migration in vitro and improves neointima formation after balloon injury in vivo. Atherosclerosis. 2006; 186: 29–37. https://doi.org/10.1016/j.atherosclerosis.2005.06.048 PMID: 16098530

52. Takahara M, Takaki A, Hiraoka S, Adachi T, Shimomura Y, Matsushita H, et al. Berberine improved experimental chronic colitis by regulating interferon-γ- and IL-17A-producing lamina propria CD4+ T cells through AMPK activation. Sci Rep. 2019; 9: 11934. https://doi.org/10.1038/s41598-019-48331-w PMID: 31417110

53. Lalvani A, Millington KA. T Cells and Tuberculosis: Beyond Interferon-γ. J Infect Dis. 2008; 197: 941–943. https://doi.org/10.1086/529049 PMID: 18419531

54. Flynn JL, Chan J, Triebold KJ, Dalton DK, Stewart TA, Bloom BR. An essential role for interferon gamma in resistance to Mycobacterium tuberculosis infection. J Exp Med. 1993; 178: 2249–2254. https://doi.org/10.1084/jem.178.6.2249 PMID: 7504064

55. Yin Y, Lian K, Zhao D, Tao C, Chen X, Tan W, et al. A Promising Listeria-Vectored Vaccine Induces Th1-Type Immune Responses and Confers Protection Against Tuberculosis. Front Cell Infect Microbiol. 2017; 7: 407. https://doi.org/10.3389/fcimb.2017.00407 PMID: 29034213

56. Rosato PC, Beura LK, Masopust D. Tissue resident memory T cells and viral immunity. Curr Opin Virol. 2017; 22: 44–50. https://doi.org/10.1016/j.coviro.2016.11.011 PMID: 27987416

57. Beura LK, Rosato PC, Masopust D. Implications of Resident Memory T Cells for Transplantation. Am J Transplant Off J Am Soc Transplant Am Soc Transpl Surg. 2017; 17: 1167–1175. https://doi.org/10.1111/ajt.14101 PMID: 27804207

58. Enamorado M, Iborra S, Priego E, Cueto FJ, Quintana JA, Martínez-Cano S, et al. Enhanced anti-tumour immunity requires the interplay between resident and circulating memory CD8+ T cells. Nat Commun. 2017; 8: 16073. https://doi.org/10.1038/ncomms16073 PMID: 28714465

59. Behr FM, Parga-Vidal L, Kragten NAM, van Dam TJP, Wesselink TH, Sheridan BS, et al. Tissue-resident memory CD8+ T cells shape local and systemic secondary T cell responses. Nat Immunol. 2020; 21: 1070–1081. https://doi.org/10.1038/s41590-020-0723-4 PMID: 32661361

60. Zundler S, Becker E, Spocinska M, Slawik M, Parga-Vidal L, Stark R, et al. Hobit- and Blimp-1-driven CD4+ tissue-resident memory T cells control chronic intestinal inflammation. Nat Immunol. 2019; 20: 288–300. https://doi.org/10.1038/s41590-018-0298-5 PMID: 30692620

61. Corrado M, Pearce EL. Targeting memory T cell metabolism to improve immunity. J Clin Invest. 2022; 132: e148546. https://doi.org/10.1172/JCI148546 PMID: 34981777

62. Coffre M, Benhamou D, Rieß D, Blumenberg L, Snetkova V, Hines MJ, et al. miRNAs Are Essential for the Regulation of the PI3K/AKT/FOXO Pathway and Receptor Editing during B Cell Maturation. Cell Rep. 2016; 17: 2271–2285. https://doi.org/10.1016/j.celrep.2016.11.006 PMID: 27880903

63. Bhaskar A, Chawla M, Mehta M, Parikh P, Chandra P, Bhave D, et al. Reengineering redox sensitive GFP to measure mycothiol redox potential of Mycobacterium tuberculosis during infection. PLoS Pathog. 2014; 10: e1003902. https://doi.org/10.1371/journal.ppat.1003902 PMID: 24497832

64. Bhaskar A, Kumar S, Khan MZ, Singh A, Dwivedi VP, Nandicoori VK. Host sirtuin 2 as an immunotherapeutic target against tuberculosis. eLife. 2020; 9: e55415. https://doi.org/10.7554/eLife.55415 PMID: 32697192

AMERICAN SOCIETY FOR MICROBIOLOGY | Microbiology Spectrum

RESEARCH ARTICLE

Biapenem, a Carbapenem Antibiotic, Elicits Mycobacteria Specific Immune Responses and Reduces the Recurrence of Tuberculosis

Isha Pahuja,[a,b] Akanksha Verma,[a] Antara Ghoshal,[a] Suparba Mukhopadhyay,[a] Anjna Kumari,[a] Aishwarya Shaji,[a] Shivam Chaturvedi,[a] Ved Prakash Dwivedi,[a] Ashima Bhaskar[a]

[a]Immunobiology Group, International Centre for Genetic Engineering and Biotechnology, New Delhi, India
[b]Department of Molecular Medicine, Jamia Hamdard University, New Delhi, India

Isha Pahuja, Akanksha Verma, and Antara Ghoshal are contributed equally to the manuscript. The author order was decided on the basis of the experiments performed.

ABSTRACT Tuberculosis (TB) still tops the list of global health burdens even after COVID-19. However, it will sooner transcend the current pandemic due to the prevailing risk of reactivation of latent TB in immunocompromised individuals. The indiscriminate misuse and overuse of antibiotics have resulted in the emergence of deadly drug-resistant variants of *Mycobacterium tuberculosis* (*M.tb*). This study aims to characterize the functionality of the carbapenem antibiotic-Biapenem (BPM) in generating long-lasting immunity against TB. BPM treatment significantly boosted the activation status of the innate immune arm-macrophages by augmenting p38 signaling. Macrophages further primed and activated the adaptive immune cells $CD4^+$ and $CD8^+$ T-cells in the lung and spleen of the infected mice model. Furthermore, BPM treatment significantly amplified the polarization of T lymphocytes toward inflammatory subsets, such as Th1 and Th17. The treatment also helped generate a long-lived central memory T-cell subset. The generation of central memory T lymphocyte subset upon BPM treatment in the murine model led to a significant curtailing in the recurrence of TB due to reactivation and reinfection. These results suggest the potentiality of BPM as a potent adjunct immunomodulator to improve host defense against *M.tb* by enriching long-term protective memory cells.

IMPORTANCE Tuberculosis (TB) caused by *Mycobacterium tuberculosis* (*M.tb*) tops the list of infectious killers around the globe. The emergence of drug-resistant variants of *M.tb* has been a major hindrance toward realizing the "END TB" goal. Drug resistance has amplified the global burden toward the quest for novel drug molecules targeting *M.tb*. Host-directed therapy (HDT) offers a lucrative alternative to tackle emerging drug resistance and disease relapse by strengthening the host's immunity. Through our present study, we have tried to characterize the functionality of the carbapenem antibiotic-Biapenem (BPM). BPM treatment significantly augmented long-lasting immunity against TB by boosting the innate and adaptive immune arms. The generation of long-lived central memory T lymphocyte subset significantly improved the disease outcome and provided sterilizing immunity in the murine model of TB. The present investigation's encouraging results have helped us depict BPM as a potent adjunct immunomodulator for treating TB.

KEYWORDS tuberculosis, immunotherapy, Biapenem, memory T-cells, reactivation, reinfection, antimicrobials, *Mycobacterium tuberculosis*, multidrug resistance

Tuberculosis (TB) is an age-old disease caused by *Mycobacterium tuberculosis* (*M.tb*) that still affects a majority of the population worldwide. TB was the leading cause of death by a single infectious agent until the COVID-19 pandemic (1, 2). The incidence

Editor John M. Atack, Griffith University

Address correspondence to Ashima Bhaskar, ashimabhaskar23@gmail.com, or Ved Prakash Dwivedi, vedprakashbt@gmail.com.

The authors declare no conflict of interest.

Received 27 February 2023
Accepted 23 May 2023
Published 5 June 2023

of the pandemic has reversed the progress in TB diagnosis and treatment to date and further aggravated the global TB burden (3).

The treatment of TB comprises a first line anti-tubercular therapy (ATT) with directly observed treatment short course (DOTS), a customary prescribed by the WHO as a TB control measure, and it consists of 4 drugs, Isoniazid, Rifampicin, Pyrazinamide, and Ethambutol. The treatment course duration runs from 6 to 8 months (4). From the duration of therapy being too prolonged that adversely affects the financial burden in the lower-income strata countries where the prevalence of TB has been very prominent, the subsequent chance of relapse of the disease by reinfection even after the cure post treatment, may cause immune dampening in the patients, meaning DOTS does not pose as a promising therapy to TB. Furthermore, the cost and duration of treatment, and the lack of proper infrastructure, often enforce the patients to stop it midway, consequently negatively impacting them and leading to drug resistance (5). The emergence of drug resistance in TB dampened the progress made in curbing the disease even more. The success of multi-drug resistant (MDR) and extensively drug resistant (XDR) tuberculosis treatments cater the use of fluoroquinolones as first line drugs and also depend on the degree of the resistance. The length of treatment for MDR and XDR TB is not defined and varies from patient to patient (6).

The infidelity of the progression of the disease also caters to the difficulty in its prophylactic measures too. The Bacille Calmette-Guerin (BCG) vaccine is the only approved chemoprophylactic measure against TB infection to date. Its efficacy is most pronounced in disseminated forms of TB in children compared to pulmonary TB in adults (7).

Beta-lactam antibiotics, broad-spectrum drugs that have been used to treat many Gram-negative bacterial infections by inhibiting the cell wall synthesis of bacteria and carve a niche in treatment against the drug-resistant bacteria. Conventionally, these beta-lactam antibiotics were not used against treating TB pertaining to the presence of an extremely active β-lactamase (BlaC) that is chromosomally encoded in *M.tb* (8). However, carbapenems, a subclass of beta-lactam antibiotics, have a unique structural composition that makes them non-susceptible to the β-lactamase activity of *M.tb* and hence a poor substrate for BlaC. This property of the carbapenems made them an efficient target for treatment against drug-resistant *M.tb* strains (8, 9). Biapenem (BPM), one of the most common commercially available carbapenems, has a potent efficacy as anti-tuberculous agent against drug-susceptible and drug-resistant *M.tb* strains compared to other carbapenems owing to its robust pharmacokinetic activities (10, 11). Recent studies show BPM exhibiting antibacterial activity and antimicrobial activity against *M.tb* in both *in vitro* and *in vivo* settings. BPM also exhibits synergy with Rifampicin, one of the first line anti-TB drug against drug-susceptible *M.tb* infections (11–13). Since most of the current ATT drugs cause severe immune dampening (14), effects of BPM on the host immune responses should be explored to project BPM as a potential candidate for ATT.

Here, we have examined the immunomodulatory actions of -BPM during *M.tb* infection *ex vivo* and *in vivo*. Our results demonstrate the efficacy of -BPM as a potent modulator of innate and adaptive immune responses. BPM regulates various host defense mechanisms aiding in combating *M.tb* infection. BPM boosted the antimicrobial activity of the macrophages by regulating ROS levels and p38 MAPK signaling. It also enhanced the expression of pro-inflammatory cytokines and co-stimulatory molecules. The activated innate immune responses upon BPM treatment played a vital role for further stimulation of the adaptive immune responses. With enhanced T cell activation, BPM treatment significantly enriched the protective T cell responses in the lungs and the spleen of *M.tb* infected mice. Moreover, BPM treatment enhanced the expression of IFN-γ and IL-17, the proinflammatory cytokines known to play a significant role in rendering protection to the host against the bacterial infection. Further immune analysis revealed enhanced T-cell memory responses in the BPM treated mice. It has been established that the central memory (T_{CM}) and effector memory (T_{EM}) T-cells play a vital role in the protection of host during recall responses (15–17). One of the major challenges associated with TB

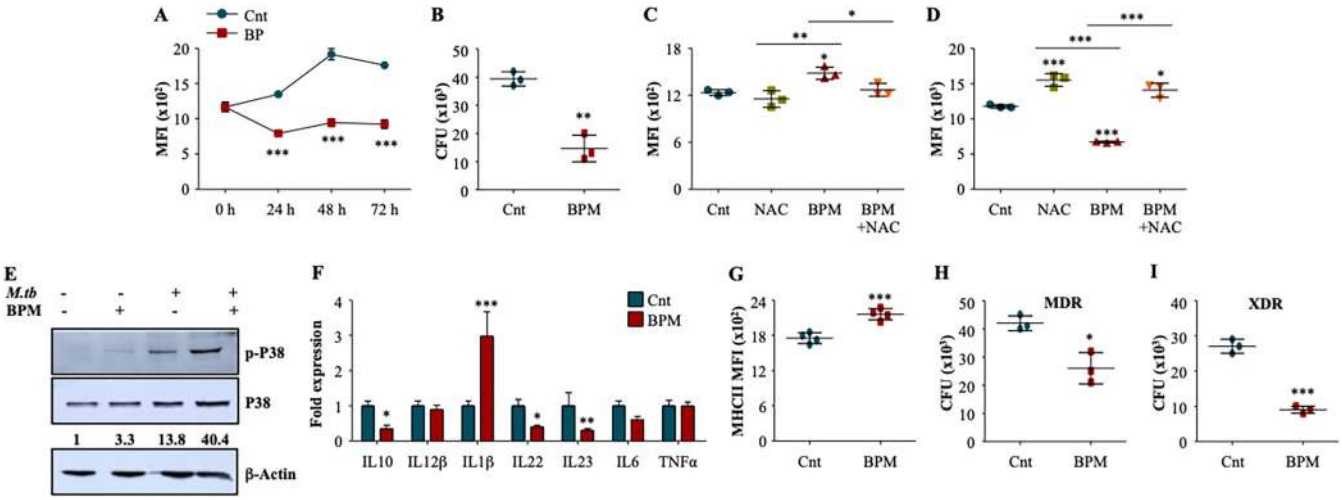

FIG 1 Biapenem augments the anti-mycobacterial activity of macrophages by modulating p38 MAPK signaling. Murine macrophages were infected with GFP expressing *M.tb* H37Rv at MOI 1:1 and treated with BPM (10 μg/mL). (A) Intracellular GFP fluorescence at different time points postinfection with and without BPM treatment. (B) Peritoneal macrophages were infected with *M.tb* H37Rv at MOI 1:10 followed by treatment with BPM (10 μg/mL) for 48 h. CFU determination at 48h post treatment. (C) and (D) Mouse peritoneal macrophages pretreated with 10 mM NAC were infected with GFP expressing *M.tb* H37Rv at an MOI of 1:1 followed by treated with 10 μg/mL BPM. (C) Intracellular ROS levels 48 h postinfection. (D) Corresponding bacterial survival post 48 h BPM and NAC treatment. (E) Western blots analysis to show the phosphorylation of P38 in uninfected and infected mouse peritoneal macrophages with or without BPM treatment for 2 h. (F) Fold change in the expression of cytokines in the infected macrophages with or without BPM treatment. (G) Expression of MHC-II on *M.tb* infected peritoneal macrophages 48 h post treatment with 10 μg/mL BPM. (H) and (I) Peritoneal macrophages were infected with *M.tb* Jal 2261 (MDR) and MYC 431 (XDR) at MOI 1:10, followed by treatment with BPM (10 μg/mL). (H) MDR and (I) XDR bacterial burden at 48 h post treatment. Data is representative of 3 independent experiments. The results shown are means $\pm$ SD (n = 3 or 4). P value * $\leq$ 0.05, ** $\leq$ 0.005, *** $\leq$ 0.0005.

prophylaxis is the persistent recurrence of the disease in the form of reactivation or reinfection; our study demonstrated that BPM plays a substantial role in reduction of this recurrence. Considering all these beneficial facets of BPM against *M.tb*, it can potentiate as an immunomodulator against TB pathogenesis and can translate to prospective aid in treatment to human patients as well.

RESULTS

Biapenem enhances antimycobacterial potential of macrophages by modulating P38 signaling pathway. BPM, a carbapenem antibiotic, has already been shown to have anti-mycobacterial potential in several studies (11, 17). It has been shown that BPM has synergistic antimycobacterial effect with rifampicin both *in vitro* and *in vivo* (12, 13). However, none of the studies explore its effect on the host immunity. To begin, we assessed the time kinetics of intra-macrophage bacterial growth in the presence of BPM. For this, mice peritoneal macrophages were infected with *M.tb* H37Rv-GFP (MOI 1:1) and treated with BPM followed by flow cytometry to determine the bacterial growth at different time points. We observed that BPM significantly induces the potential of macrophages to restrict the mycobacterial growth in time dependent manner (Fig. 1A). Further, CFU determination at 48 h postinfection with *M.tb* H37Rv (MOI 1:10) indicated similar results (Fig. 1B). Macrophages employ several defense mechanisms to restrict the growth of the pathogens, such as the generation of reactive oxygen species (ROS) and reactive nitrogen species (RNS) (18) .We observed that BPM treatment induced significant levels of ROS in the infected macrophages as observed by an increase in the CellROX fluorescence (Fig. 1C), which was reduced upon treatment with the antioxidant, N-acetylcysteine (NAC) (19). Furthermore, NAC co-treatment abolished the anti-mycobacterial potential of BPM indicating ROS generation as one of the major mechanisms by which BPM exerts its effect (Fig. 1D).

Since ROS is known to induce multiple intracellular signaling pathways (20–22), we analyzed the activation status of MAPK pathway upon BPM treatment. We observed that BPM activates p38 signaling (Fig. 1E), which further led to the induction of proinflammatory cytokines (Fig. 1F) that mediate bacterial killing and are also required for T cell differentiation toward the protective Th1 and Th17 cells (23–26). Further, BPM

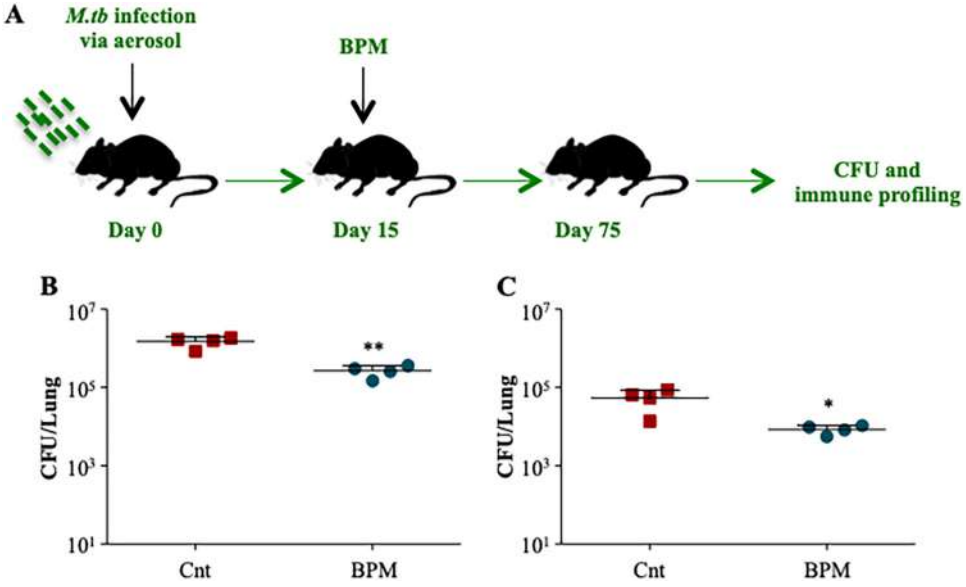

FIG 2 Biapenem treatment restricts the mycobacterial growth *in vivo*. (A) Schematic representation of mice model used in the study. Bacterial burden in the (B) lungs and (C) spleen of BPM treated animals 75 days postinfection. Data is representative of 2 independent experiments. The data values represent mean ± SD ($n = 4$). *, $P < 0.05$, **, $P < 0.005$, ***, $P < 0.0005$.

treatment led to enhanced expression of MHCII on the infected macrophages which may aid in T cell activation (Fig. 1G) (27, 28). Lastly, BPM displayed significant anti-tubercular activity against drug-resistant clinical isolates of *M.tb* (Fig. 1H and I). Collectively, our *ex vivo* data indicates that BPM treatment positively induces the activation of macrophages and stimulates the pro-inflammatory environment to mediate the host resistance to TB.

Biapenem restricts the mycobacterial growth in mice. To corroborate our *ex vivo* findings, we performed an *in vivo* experiment wherein C57BL/6 mice were infected with *M.tb* H37Rv through low dose aerosol infection model. Group of animals were either kept untreated or were treated with BPM (5 mg/kg) for 60 days followed by determination of bacterial burden and immune profiling (Fig. 2A). BPM treatment significantly lowered the bacillary load in the lungs (Fig. 2B) and the spleen (Fig. 2C) of *M.tb* infected mice compared to the untreated control group as reported earlier.

Biapenem activates innate immune cells during TB. As observed in Fig. 1, BPM treatment modulated intracellular signaling to activate macrophages. To further evaluate the potential of BPM in activating innate immunity *in vivo*, macrophage activation was assessed in infected and BPM treated lungs and spleen. Gating strategy employed in this study is depicted in Fig. S1. While no significant increase in the $CD11b^+$ and $CD11c^+$ cells was observed in the spleen of infected animals (Fig. 3A and B), BPM significantly enhanced the percentage of $CD11c^+$ cells in the infected lungs (Fig. 3C and D). Henceforth, the co-stimulatory and activation markers CD80, CD86, and CD40 were analyzed in the BPM treated infected lung and spleen to measure the activation of innate cells. There was a substantial increase in the expression of CD86 and CD40 on $CD11b^+$ and $CD11c^+$ cells upon BPM treatment in the infected spleen (Fig. 3E to G), while no significant increase in the expression of CD80 (Fig. 3H) was observed. Further, BPM treated innate cells in the lungs showed significant enhancement in the expression of CD80 and CD40 with no effect on CD86 (Fig. 3J and L). Altogether, this data suggests that BPM induces an innate immune response via the activation of macrophages and dendritic cells in the lungs and the spleen of infected mice, which is required to activate adaptive immunity.

Biapenem induces long-lasting protective T cell immunity by enriching the pool of central memory T cells in mice. Host immunity plays a critical role in restricting the dissemination of *M.tb* and therefore, only a small population develops active TB despite being latently infected. A critical balance of immune responses is required

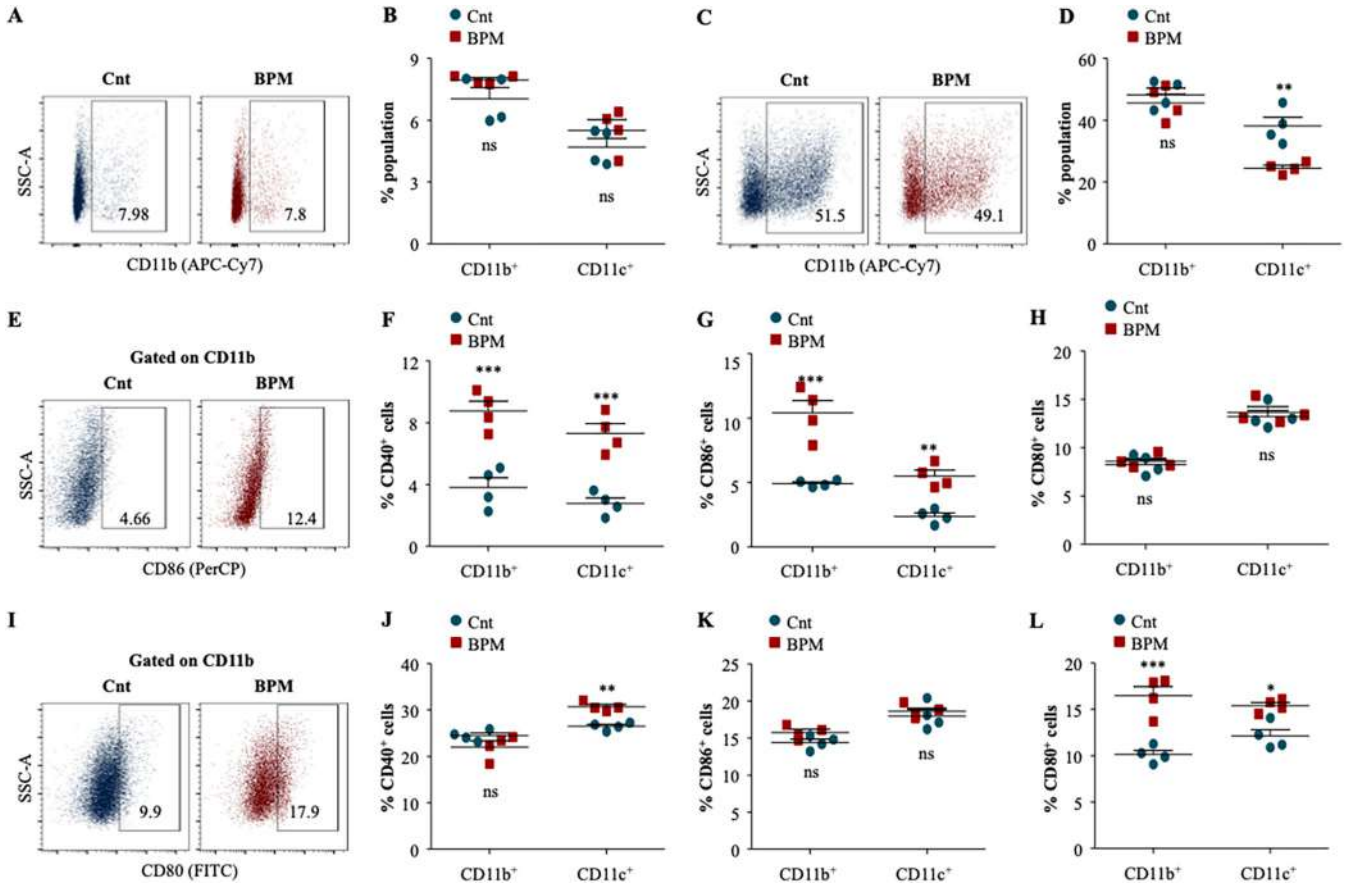

FIG 3 Biapenem treatment induces innate immune activation crucial for the activation of adaptive immunity in *in vivo* settings. Single cell suspensions generated from the infected lungs and spleen were *ex vivo* stimulated with *M.tb* complete soluble antigen (CSA) for overnight followed by surface staining with antibodies against CD11b (APCCy7), CD11c (APC), CD80 (FITC), CD86 (PerCPCy5.5), and CD40 (PE) and subjected to flow cytometry. (A) Representative dot plots and the percentage of (B) $CD11b^+$ and $CD11c^+$ cells in the infected and BPM treated spleen. (C) Representative dot plots depicting the percentage of (D) $CD11b^+$ and $CD11c^+$ cells in the infected and BPM treated lung. (E) Representative dot plots and the percentage of (F) $CD40^+$, (G) $CD86^+$, and (H) $CD80^+$ cells in the $CD11b_+$ and $CD11c^+$ splenic cells. (I) Representative dot plots and the percentage of (J) $CD11b^+CD40^+$ and $CD11c^+CD40^+$ cells, (K) $CD11b^+CD86^+$ and $CD11c^+CD86^+$ cells, and (L) $CD11b^+CD80^+$ and $CD11c^+CD80^+$ cells in the lungs of infected and BPM treated animals. Data is representative of 2 independent experiments. The data values represent mean ± SD ($n = 4$). *, $P < 0.05$, **, $P < 0.005$, ***, $P < 0.0005$.

to contain the infection. It has been largely established that IFN-γ-producing $CD4^+$ T cells provides protective immunity against TB and any defect in Th1 signaling leads to the unrestricted growth of *M.tb* (29, 30). Moreover, IL-4 producing Th2 cells assists in disease progression (31, 32). Recently, we and others have established that Th17 cells largely provide protection during secondary infection synergistically with Th1 cells (33–35). In the previous result, we established that BPM treatment significantly induces the pro-inflammatory signaling in macrophages, which are very critical to activate adaptive immunity. Therefore, we extended our interest in profiling the T cell responses after BPM treatment. With no change in the percentage of $CD4^+$ and $CD8^+$ T-cells (Fig. 4A and B), the expression of activation marker CD69 was significantly enhanced in the splenic $CD4^+$ and $CD8^+$ T cells (Fig. 4C and D).

Furthermore, BPM treatment significantly induced the IFN-γ producing T cell (Fig. 4E and F) with no change in the IL-17 producing T cell (Fig. 4G and H) responses in the spleen of infected animals.

Strong pro-inflammatory innate and adaptive immunity is not sufficient to achieve sterile immunity. Long-term sustained immune responses in terms of memory cells are critically required to control the infection as well as to reduce the host vulnerability to disease reinfection and reactivation (15, 16, 36). Upon antigen encounter, T naive cells differentiate into central memory T-cells (T_{CM}) and effector memory T-cells (T_{EM}). T_{EM} cells are short-lived, have limited proliferative capacity, and participate in the immediate

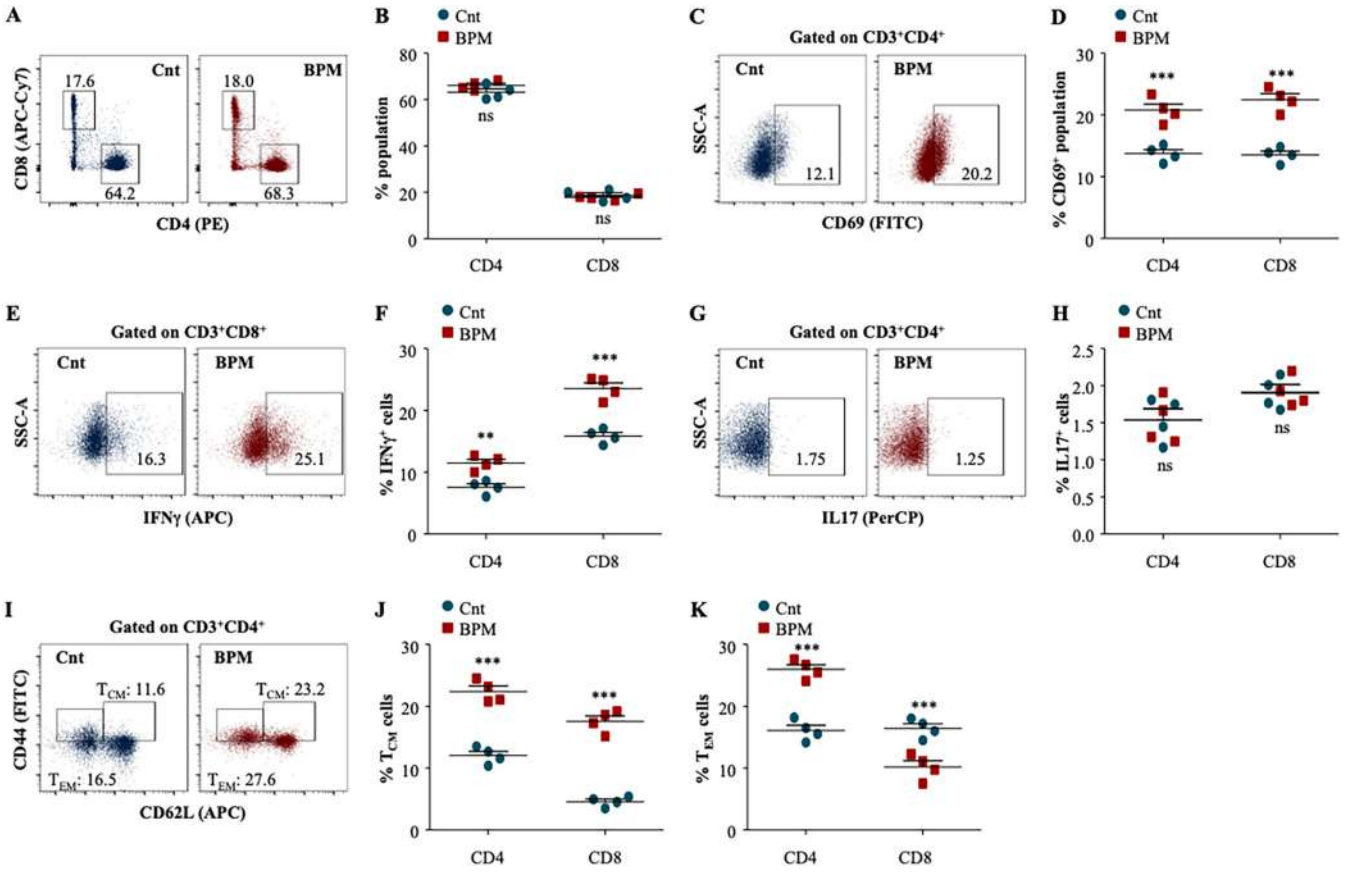

FIG 4 Biapenem treatment augments T cell responses required for long-term protection against tuberculosis in the spleen of infected mice. (A) to (D) *Ex vivo* stimulated splenocytes were surface stained with α-CD3 (Pacific Blue), α-CD4 (PE), α-CD8 (APCCy7), and α-CD69 (FITC) followed by flow cytometry. (A) Representative dot plots and (B) the percentage of $CD4^+$ and $CD8^+$ T cells in the infected spleen. (C) Representative dot plots and (D) the percentage of $CD4^+CD69^+$ and $CD8^+CD69^+$ T cells in the spleen of infected mice. (E) to (H) *Ex vivo* stimulated splenocytes were treated with monensin and brefeldin A for 2 h and surface stained with α-CD3 (Pacific Blue), α-CD4 (PE), and α-CD8 (APCCy7) followed by intracellular staining with α-IFNγ (APC) and α-IL-17 (PerCP). (E) Representative dot plots and (F) the percentage of $CD4^+IFN\gamma^+$ and $CD8^+IFN\gamma^+$ T cells in the spleen of infected and BPM treated mice. (F) Representative dot plots and (G) the percentage of $CD4^+IL\text{-}17^+$ and $CD8^+IL\text{-}17^+$ T cells in the spleen of infected and BPM treated mice. (I) to (K) *Ex vivo* stimulated splenocytes were surface stained with α-CD3 (Pacific Blue), α-CD4 (PE), α-CD8 (APCCy7), α-CD62L (APC), and α-CD44 (FITC) followed by flow cytometry. (I) Representative dot plots and (J) the percentage of $CD4^+/CD8^+$ T_{CM} cells ($CD62L^{HI}CD44^{HI}$) and (K) $CD4^+/CD8^+$ T_{EM} ($CD62L^{LO}CD44^{LO}$) cells in the infected and BPM treated spleen of the mice. Data is representative of 2 independent experiments. The data values represent mean $\pm$ SD (n = 4). *, $P < 0.05$, **, $P < 0.005$, ***, $P < 0.0005$.

elimination of the pathogens whereas, T_{CM} cells can effectively proliferate and further gives rise to T_{EM} cells to control the infection. We assessed the impact of BPM treatment on different T cell memory subsets within the $CD4^+$ and $CD8^+$ T cell population (Fig. 4I). We observed a significant increase in the percentage of $CD4^+$ and $CD8^+$ T_{CM} cells (Fig. 4J) in the spleen of infected animals. While BPM treatment increased $CD4^+$ T_{EM} cells, $CD8^+$ T_{EM} cells were decreased upon BPM treatment in the spleen of infected animals (Fig. 4K).

BPM treated and *M.tb* infected lungs were also analyzed T cell mediated immune responses. BPM treatment significantly increased the percentage of $CD4^+$ T cells with no effect on the $CD8^+$ T cells (Fig. 5A and B). However, treatment with BPM significantly enhanced the percentage activation of $CD4^+$ and $CD8^+$ T cells as evidenced by the expression of CD69 on the surface of $CD4^+$ and $CD8^+$ T cells in the lung of infected animals (Fig. 5C and D). Moreover, IFNγ producing $CD4^+$ and $CD8^+$ T cells and IL-17 producing $CD4^+$ T cells were also enriched in the lung of the BPM treated animals (Fig. 5E to H). Furthermore, BPM treatment significantly induced the percentage of $CD8^+$ T_{CM} with modest effect on $CD4^+$ T_{CM} cells (Fig. 5I and K). However, there was significant increase in the percentage of $CD4^+T_{EM}$ and $CD8^+$ T_{EM} in the lung of infected animals (Fig. 5L). Altogether, these results strongly suggest that BPM treatment strengthens the long-lasting protective immunity in the *M.tb* infected animals.

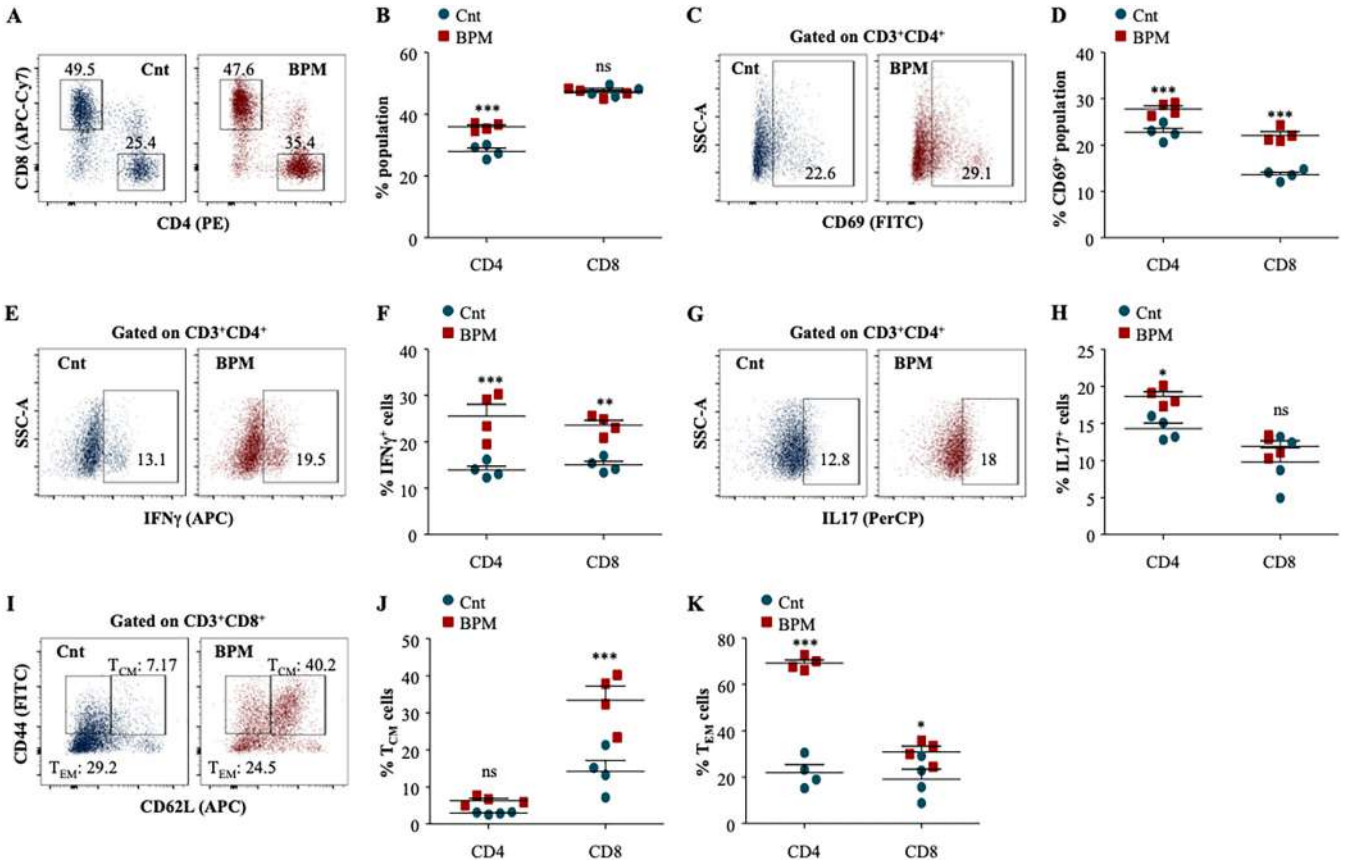

FIG 5 Biapenem treatment instigates long-term protective T cell immunity against tuberculosis in the lung of mice. (A) to (D) *Ex vivo* stimulated lung cells were surface stained with α-CD3 (Pacific Blue), α-CD4 (PE), α-CD8 (APCCy7), and α-CD69 (FITC) followed by flow cytometry. (A) Representative dot plots and (B) the percentage of $CD4^+$ and $CD8^+$ T cells in the infected lungs. (C) Representative dot plots and (D) the percentage of $CD4^+CD69^+$ and $CD8^+CD69^+$ T cells in the lungs of infected mice. (E) to (H) *Ex vivo* stimulated lung cells were treated with monensin and brefeldin A for 2 h and surface stained with α-CD3 (Pacific Blue), α-CD4 (PE), and α-CD8 (APCCy7) followed by intracellular staining with α-IFNγ (APC) and α-IL-17 (PerCP). (E) Representative dot plots and (F) the percentage of $CD4^+IFN\gamma^+$ and $CD8^+IFN\gamma^+$ T cells in the lungs of infected and BPM treated mice. (F) Representative dot plots and (G) the percentage of $CD4^+IL\text{-}17^+$ and $CD8^+IL\text{-}17^+$ T cells in the lungs of infected and BPM treated mice. (I) to (K) *Ex vivo* stimulated lungs were surface stained with α-CD3 (Pacific Blue), α-CD4 (PE), α-CD8 (APCCy7), α-CD62L (APC), and α-CD44 (FITC) followed by flow cytometry. (I) Representative dot plots and (J) the percentage of $CD4^+/CD8^+$ T_{CM} cells ($CD62L^{HI}CD44^{HI}$) and (K) $CD4^+/CD8^+$ T_{EM} ($CD62L^{LO}CD44^{LO}$) cells in the infected and BPM treated lungs. Data is representative of 2 independent experiments. The data values represent mean $\pm$ SD ($n = 4$). *, $P < 0.05$, **, $P < 0.005$, ***, $P < 0.0005$.

Biapenem treatment reduces the extent of TB recurrence. The current available antituberculosis therapy fails to provide 100% sterilization. Moreover, due to the severe immune dampening side effects of the therapy, the host is left vulnerable to disease reinfection and relapse (14, 37, 38). Central memory T cells play vital roles in providing long-lasting protection and reduces the host vulnerability to TB reactivation and reinfection. Since BPM treatment positively modulates the host immune responses against *M.tb* and enriches the central memory T cells in *M.tb* infected mice, we evaluated the potential of BPM to be an adjunct to the current treatment regime. The impact of BPM treatment against recurrent infection and re-activation of TB was also analyzed. C57BL/6 mice were infected with *M.tb* H37Rv through low dose aerosol infection model and after 15 days these mice were treated with either INH+RIF (Cnt group) or INH+RIF+BPM (treatment group) for the next 60 days, followed by CFU analysis (Fig. 6A). After 30 days rest, the mice were re-challenged with *M.tb* H37Rv through low dose aerosol infection model for reinfection studies (Fig. 6A). For re-activation, the rested mice were treated with immunosuppressive drug dexamethasone for 30 days (Fig. 6A).

A synergistic effect in the bacterial reduction was observed in the infected mice treated with BPM along with INH/RIF, indicating that BPM co-treatment extensively enhances the anti-tubercular potential of present available antituberculosis therapy (Fig. 6B and C).

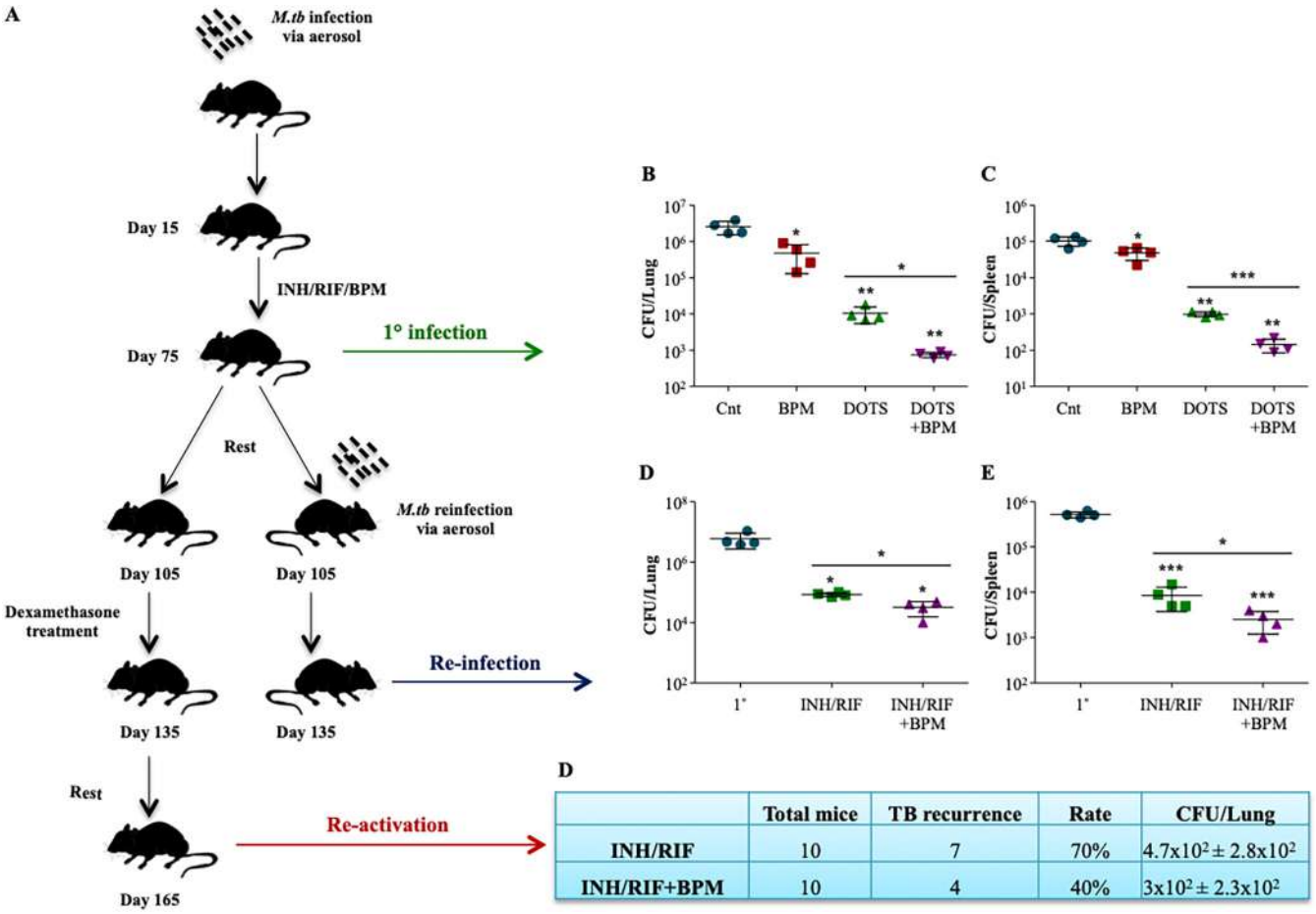

D

	Total mice	TB recurrence	Rate	CFU/Lung
INH/RIF	10	7	70%	$4.7x10^2 \pm 2.8x10^2$
INH/RIF+BPM	10	4	40%	$3x10^2 \pm 2.3x10^2$

FIG 6 Biapenem reduces the recurrence of tuberculosis reinfection and reactivation. (A) Schematic representation of primary infection, re-infection, and re-activation mice model used in the study. Bacterial burden in the (B) lungs and (C) spleen of BPM and INH/RIF treated animals 75 days postinfection. Bacterial burden in the (D) lungs and (E) spleen of BPM and INH/RIF treated and reinfected animals. (F) Rate of disease relapse with and without BPM treatment in re-activation group. Data is representative of 2 independent experiments. The data values represent mean ± SD (n = 4 to 10). *, $P < 0.05$, **, $P < 0.005$, ***, $P < 0.0005$.

The INH/RIF/BPM treated and reinfected mice displayed increased anti-tubercular immunity as evidenced by a significant reduction in the bacterial burden in the lungs (Fig. 6D) and the spleen (Fig. 6E) of these mice compared to the group that received only INH/RIF. BPM co-treatment also reduced the TB reactivation rate from 70% to 40% (Fig. 6F). Overall, these results signify the potential of BPM as an adjunct immunomodulator for TB therapy.

DISCUSSION

The current regime for TB treatment has been proven to dampen the host's immune system, which allows partial reduction of bacterial burden in the infected individuals (39). This further leads to the emergence of drug-resistant TB, such as MDR, XDR, and now recently emerging TDR (40). Therefore, researchers are now pacing toward immunomodulatory therapy that can efficiently control mycobacterial infection.

BPM is a wide-spectrum anti-bacterial drug that has been shown to impart substantial immunity against drug-susceptible TB in the *in vitro* and *in vivo* mice models. It acts synergistically with rifampicin and thereby confers better protection against *M.tb* (12). In this study, we have tried to evaluate the effect of BPM on the host immune system and understand the mechanism of action of BPM in the reduction of *M.tb* load.

Innate immune cells like macrophages are the first line of defense against *M.tb*. These immune cells subsequently help prime the adaptive immune cells like T cells to improve the disease outcome and provide long-term immunity (41). ROS is one of the

well-studied features employed by macrophages to combat intracellular pathogens by activating a plethora of signaling pathways that ultimately result in the generation of a pro-inflammatory milieu for pathogen elimination (42). Consistent with this understanding, BPM treatment in peritoneal macrophages significantly enhanced ROS generation and activation of the p38 signaling pathway, which is known to induce pro-inflammatory cytokines like IL-1β. It has been reported that IL-1β from innate cells like macrophages and the dendritic cell can prime T cells and result in their activation and differentiation (43). Various studies and models have postulated that the balance between pro-inflammatory and anti-inflammatory cytokines is necessary to culminate the bacterial progression in infected individuals (44). Assorted reports suggest that IFNγ producing T cells provide immunity against TB, and thereby T cells priming is essential to impart immunity against the bacteria (45).

To substantiate our encouraging *ex vivo* findings, we further assessed the impact of BPM on the modulation of the host immune system. We observed that upon BPM treatment, the innate cells expressing co-stimulatory and activation markers, such as CD80, CD86, and CD40, were enhanced at the primary site of infection, i.e., lungs. These observations correlate that upon *M.tb* infection, BPM enhances the activation of dendritic cells and macrophages to increase the antigen presentation to the T cells leading to enhanced T cell activation. Indeed, BPM treatment increased the activation of $CD4^+$ and $CD8^+$ T cells in the lungs and the spleen of the *M.tb* infected mice as evidenced by the increase in the expression of CD69. Further, these T cells demonstrated enhanced production of the pro-inflammatory cytokine, IFN-γ, which is known to have a protective role against *M.tb* (46). Anther pro-inflammatory cytokine, IL-17, which is known to impart long-term immunity (47), was significantly increased in the BPM treated mice.

Classically, it has been acknowledged that long-term memory plays a crucial role in protection against secondary infection with *M.tb*. Upon antigen encounter, Naïve T cells differentiate into central memory T cells (T_{CM}), which are further differentiated in secondary lymphoid organs into effector memory cells (T_{EM}) (48, 49). Therefore, we evaluated the potential of BPM in modulating T cell memory responses to mediate long-term memory against *M.tb*. Recently we and others have shown how antimycobacterial compounds elicit *M.tb* specific long-term immunity (50–52). Here, again, we observed that BPM boosted the memory responses in both the lung and the spleen of infected animals.

The anti-tubercular drugs are known to have an immune dampening effect and fail to provide complete sterility. Therefore, we evaluated BPM as an adjunct therapy with DOTS and observed that BPM co-administration significantly enhanced the anti-tubercular potential of current front-line anti-TB drugs, INH, and RIF. This was also supported by our findings that the extent of TB recurrence due to reinfection and reactivation was also reduced significantly with BPM as an adjunct.

Apart from its classical role as an anti-tubercular drug, our findings suggest that BPM also functions as an immunomodulator. Collectively, it can be proposed that BPM possesses broad-spectrum activities and thus can be projected as a potential adjunct immunotherapeutic against TB (Fig. 7).

MATERIALS AND METHODS

Ethics statement. Mice were procured from the ICGEB animal facility and the experiments were performed as per the instructions specified by the Institutional Animal Ethics Committee of the International Centre for Genetic Engineering and Biotechnology (ICGEB, New Delhi, India) together with the Department of Biotechnology (DBT) standards (Government of India) (Approval ID: ICGEB/IAEC/18092021/IMB-19). The animals utilized were virtuously sacrificed by asphyxiation with carbon dioxide in accordance with institutional and DBT practices.

Mice. C57BL/6 mice of 6 to 8 weeks were nurtured and maintained in the Animal facility at ICGEB, New Delhi, India. Mice were procured for the experimental strategy from the facility.

Bacterial strains. Mid log phase cultures of *Mtb* (H37Rv and Rv-GFP), MDR (JAL 2261) and XDR (MYC 431) strains were used for the study. For culturing of the mycobacterial strains 7H9 (Middlebrooks, Difco, 462) medium supplemented with 10% OADC (Oleic acid, albumin, dextrose, and catalase; 463 Difco),

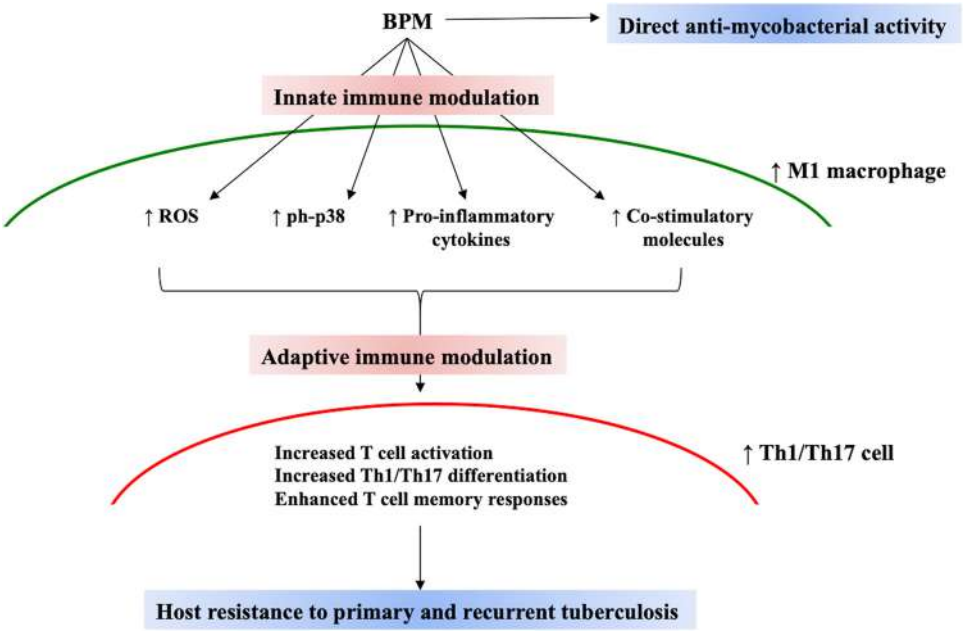

FIG 7 Proposed mechanism of action of BPM during *M.tb* infection. As a carbapenem, BPM has direct anti-mycobacterial effect. BPM also exerts immunomodulatory effects on the innate and adaptive immune arm of the host. In macrophages, BPM treatment leads to increased levels of ROS, p38 activation, pro-inflammatory cytokine secretion, and co-stimulation indicative of M1 macrophage phenotype. This further leads to positive modulation of T cells in terms of activation and Th1/Th17 environment, which is beneficial for the host.

0.05% Tween 80, and 0.2% glycerol were used. Bacterial stocks prepared in 20% glycerol were cryopreserved at −80°C, and these stocks were further used for all the infection experiments in the study.

Isolation of mouse peritoneal macrophages. C57/BL6 mice aged 6 to –8 weeks were administered intraperitoneally with sterile thioglycolate (2 mL; Brewer modified, BBL, BD Biosciences: 4% wt/vol in water). Post 5 days, macrophages were isolated from the peritoneal lavage by flushing them with ice-chilled PBS. The cells were pelleted down and resuspended in RPMI 1640 media supplemented with 10% heat-inactivated fetal calf serum and 1% antibiotic (Penicliin-Streptomycin). Cell viability was determined by trypan blue dye staining using a hemocytometer. Cells were seeded and incubated overnight at 37°C and 5% CO_2. Non-adherent cells were washed off using sterile 1X PBS, and the adherent macrophage monolayer was further infected with 1:1 MOI of Rv-GFP and 1:10 MOI of H37Rv.

***Ex vivo* infection and CellROX assay.** Mouse peritoneal macrophages were used for *ex vivo* experimental procedures. Mid log phase cultures were maintained from bacterial cryostocks. Single cell suspension of the bacterial cultures was prepared by passing it through a 23 $^1/_2$ gauge syringe 10, followed by a 26 $^1/_2$-gauge syringe. Macrophages were infected with H37Rv and H37Rv-GFP at MOI 1:10 and 1:1, respectively. Post 4 h of infection, cells were washed twice with 1X PBS to terminate *M.tb* infection. The cells were then treated with 10 mM NAC or 10 μg/mL BPM and incubated at 37°C and then analyzed for intracellular ROS and bacterial burden. CellROX Deep Red Reagent (ThermoFisher Scientific) was used to estimate the ROS levels as per the protocol supplied by the manufacturer.

***In vivo* mice infection and CFU determination.** Mice were infected via aerosol route with a drug-susceptible strain of *M.tb* (H37Rv) to deliver 110 viable bacilli to mouse lungs. Madison aerosol chamber (University of Wisconsin) with its pre-adjusted nebulizer containing 15 mL of bacterial single cell suspension was used for infection. Mice from each group were sacrificed at indicated time points to determine the bacterial load. For CFU enumeration, harvested lung and spleen from designated groups of mice were homogenized in sterile 1X PBS and then plated on 7H11 Middlebrooks (Difco) plates containing 0.05% Tween 80, 10% oleic acid, albumin, dextrose, and catalase (OADC) (Difco) in different dilutions. The plates were then incubated at 37°C and the colonies were examined after 3 weeks.

Drug delivery. For *ex vivo* experiments, cells were treated with 10 μg/mL of BPM (Sigma-Aldrich). Furthermore, for long-term mice studies, 5 mg/kg of BPM dissolved in water was administered intraperitoneally for 45 days thrice a week, and the control group received only the vehicle. A total of 100 mg/L of INH and 60 mg/L RIF was given in drinking water which was replaced on alternative days.

Protein isolation and Western blotting. Peritoneal macrophages seeded at a density of 1 $\times$ 10^6cells/mL were infected with H37Rv at an MOI of 1:10. After 2 h of infection, cells were washed twice with 1X PBS to terminate the *M.tb* infection. The infected cells or uninfected cells were treated with or without 10uM of BPM for 2 h. Post 2 h of treatment, RIPA lysis buffer (50 mM Tris, pH 8.0, 150 mM NaCl, 1.0% NP-40, 0.5% Sodium deoxycholate, and 0.1% SDS) containing 1X protease inhibitor cocktail was used to prepare whole-cell lysates. Post centrifugation of lysate at 13,000 $\times$ *g*, the aqueous layer was removed and quantified for protein using Bradford reagent. Protein samples were electrophoresed using 10% polyacrylamide gel (SDS-PAGE) and electroblotted on a nitrocellulose membrane. The nitrocellulose membrane

Table 1 The primer sequences used in the study

Primer	Sequence (5′–3′)
IL-10 Forward Primer	CATGGGTCTTGGGAAGAGAA
IL-10 Reverse Primer	AACTGGCCACAGTTTTCAGG
IL-12β Forward Primer	AAGGAACAGTGGGTGTCCAG
IL-12β Reverse Primer	GGAGACACCAGCAAAACGAT
IL-1β Forward Primer	CCCAAGCAATACCCAAAGAA
IL-1β Reverse Primer	GCTTGTGCTCTGCTTGTGAG
IL-22 Forward Primer	ATGAGTTTTTCCCTTATGGGGAC
IL-22 Reverse Primer	GCTGGAAGTTGGACACCTCAA
IL-23 Forward Primer	AATAATGTGCCCCGTATCCA
IL-23 Reverse Primer	AGGCTCCCCTTTGAAGATGT
IL-6 Forward Primer	CCGGAGAGGAGACTTCACAG
IL-6 Reverse Primer	TCCACGATTTCCCAGAGAAC
TNF-α Forward Primer	TAGCCAGGAGGGAGAACAGA
TNF-α Reverse Primer	TTTTCTGGAGGGAGATGTGG
β-Actin Forward Primer	GCTGGAAGTTGGACACCTCAA
β-Actin Reverse Primer	CCAGTTGGTAACAATGCCATGT

was blocked using 5% BSA solution in PBST (PBS and 0.1% Tween 20) for 2 h. After blocking, the membrane was probed with respective antibodies from CST overnight at 4°C. Blots were developed using Chemiluminescent HRP substrate (ECL, Millipore) and visualized on ImageQuant LAS 500.

RNA isolation and qPCR. Cells were lysed using TRIzol reagent and whole RNA was extracted by the standard RNA isolation protocol. The cDNA was synthesized from isolated RNA using the iScript cDNA synthesis kit. Bio-Rad Real-time thermal cycler was further used to set up the reactions using SYBR green Master (Bio-Rad) according to the manufacturer's protocol. The primer sequences used in the study are given in Table 1.

Reinfection and reactivation assessment. To determine the vulnerability of *M.tb* infection, mice models were infected with low dose aerosol infection of the H37Rv strain. This was followed by INH (0.1g/L) and/RIF (0.06g/L) treatment for 60 days followed by 30 days' rest. During reactivation experiments, mice were given dexamethasone (5 mg/kg) intraperitoneally, thrice a week for 30 days followed by euthanizing at indicated time points to examine immunological response and bacterial burden. For reinfection studies, another group was challenged with *M.tb*. Post 30 days of infection, the mice were sacrificed to determine the bacterial burden.

Flow cytometry. Single cell suspension of lung and spleen were prepared from mice of different groups by macerating using frosted slides in ice-cold RPMI 1640 (HyClone) supplemented with 10% FBS. For comprehensible analysis of isolated cell population RBCs were further lysed by RBC lysis buffer with 10% RPMI 1640. A total of 1×10^6 cells per well were seeded in 12-well plates for staining experiment. For surface staining, cells were *ex vivo* stimulated with 10 μg/mL of H37Rv complete soluble antigen (CSA). Eventually, 0.5 μg/mL Brefeldin A and 0.5 μg/mL of Monensin solution (BioLegend) were added prior to the last 4 h of culture at 37°C and 5% CO_2. After washing the cells twice with FACS buffer (PBS + 3% FBS) and staining with the respective to the surface markers, cell fixation was done with 100 μL fixation buffer (Biolegend) for 30 min. For intracellular staining, 1X permeabilizing buffer (Biolegend) was used to internalize the antibodies and then stained with fluorescently labeled anti-cytokine antibodies. For non-fluorochrome labeled antibodies, secondary antibody tagged with Alexa Fluor 488 was employed. Acquisition was completed by flow cytometry (BD LSRFortessa Cell Analyzer - Flow Cytometers, BD Biosciences) followed by data analysis via FlowJo (Tree Star).

Antibodies. Antibodies used in the studies are mentioned below:

Anti-Mouse: CD3-Pacific Blue, CD4-PE, CD8-APCCy7, CD69-FITC, CD44-FITC, CD62L-APC, IFNγ-APC, IL-17-PECy7, CD11b-APCCy7, CD11c-APC, CD80-FITC, CD86-PerCPCy5.5, CD40-PE, CD4-APC, and CD4-FITC from Biolegend, USA.

Anti-mouse: p38, ph-p38 and β-Actin from Cell Signaling Technology.

Statistical analysis. GraphPad Prism Software was used to evaluate the executed experimental data and the significant variation among the group was analyzed by 2 tailed unpaired Student's *t* test or 1-way ANOVA. *, $P < 0.05$, **, $P < 0.005$, ***, $P < 0.0005$.

Data availability. All data are contained within the manuscript.

SUPPLEMENTAL MATERIAL

Supplemental material is available online only.

SUPPLEMENTAL FILE 1, DOCX file, 0.2 MB.

ACKNOWLEDGMENTS

We acknowledge the support of the DBT-supported Tuberculosis Aerosol Challenge Facility at the International Centre for Genetic Engineering and Biotechnology (ICGEB), New Delhi, India, and their staff in accomplishing this work. IP is the recipient of Senior

Research Fellowship from Central Council of Research in Homeopathy (CCRH), Ministry of Ayush, Government of India. A.V., A.G., and A.S. are the recipient of Junior Research Fellowship from Department of Biotechnology (DBT), Government of India. S.M. is the recipient of Junior Research Fellowship from University Grants Commission (UGC), Government of India. V.P.D. is also recipient of an Early Career Research Award from Science and Engineering Research Board (SERB), Department of Science and Technology, Government of India. A.B. is the recipient of HGK-IYBA Fellowship from Department of Biotechnology, Government of India and Women Excellence Award Science and Engineering Research Board (SERB), Department of Science and Technology, Government of India. We also acknowledge the funding support from ICGEB, New Delhi, India.

V.P.D. and A.B. conceptualized and designed the study. I.P., A.V., A.G., S.M., A.K., and A.S. acquired the data. I.P., A.V., A.G., S.C., V.P.D., and A.B. analyzed and interpreted the data. I.P., A.V., A.G., S.M., S.C., V.P.D., and A.B. drafted the article. V.P.D. and A.B. approved the final version of the article.

There is no specific funding for this work.

We declare that we have no conflicts of interest with the contents of this article.

REFERENCES

1. Kyu HH, Maddison ER, Henry NJ, Ledesma JR, Wiens KE, Reiner R, Biehl MH, Shields C, Osgood-Zimmerman A, Ross JM, Carter A, Frank TD, Wang H, Srinivasan V, Agarwal SK, Alahdab F, Alene KA, Ali BA, Alvis-Guzman N, Andrews JR, Antonio CAT, Atique S, Atre SR, Awasthi A, Ayele HT, Badali H, Badawi A, Barac A, Bedi N, Behzadifar M, Behzadifar M, Bekele BB, Belay SA, Bensenor IM, Butt ZA, Carvalho F, Cercy K, Christopher DJ, Daba AK, Dandona L, Dandona R, Daryani A, Demeke FM, Deribe K, Dharmaratne SD, Doku DT, Dubey M, Edessa D, El-Khatib Z, Enany S, et al. 2018. Global, regional, and national burden of tuberculosis, 1990–2016: results from the Global Burden of Diseases, Injuries, and Risk Factors 2016 study. Lancet Infect Dis 18:1329–1349. https://doi.org/10.1016/S1473-3099(18)30625-X.
2. Alene KA, Wangdi K, Clements ACA. 2020. Impact of the COVID-19 pandemic on tuberculosis control: an overview. TropicalMed 5:123. https://doi.org/10.3390/tropicalmed5030123.
3. WHO. 2021. Global tuberculosis report 2021. https://www.who.int/publications-detail-redirect/9789240037021. Accessed 2 June 2022.
4. WHO. 1999. What is DOTS? A guide to understanding the WHO-recommended TB control strategy known as DOTS. https://apps.who.int/iris/bitstream/handle/10665/65979/WHO_CDS_CPC_T?sequence=1. Accessed 30 August 2022.
5. Laurenzi M, Ginsberg A, Spigelman M. 2007. Challenges associated with current and future TB treatment. Infect Disord Drug Targets 7:105–119. https://doi.org/10.2174/187152607781001817.
6. Gandhi NR, Nunn P, Dheda K, Schaaf HS, Zignol M, van Soolingen D, Jensen P, Bayona J. 2010. Multidrug-resistant and extensively drug-resistant tuberculosis: a threat to global control of tuberculosis. Lancet 375:1830–1843. https://doi.org/10.1016/S0140-6736(10)60410-2.
7. Liu J, Tran V, Leung AS, Alexander DC, Zhu B. 2009. BCG vaccines: their mechanisms of attenuation and impact on safety and protective efficacy. Hum Vaccin 5:70–78. https://doi.org/10.4161/hv.5.2.7210.
8. Hugonnet JE, Tremblay LW, Boshoff HI, Barry CE, Blanchard JS. 2009. Meropenem-clavulanate is effective against extensively drug-resistant *Mycobacterium tuberculosis*. Science 323:1215–1218. https://doi.org/10.1126/science.1167498.
9. Zhang D, Wang Y, Lu J, Pang Y. 2016. *In vitro* activity of β-lactams in combination with β-lactamase inhibitors against multidrug-resistant *Mycobacterium tuberculosis* isolates. Antimicrob Agents Chemother 60:393–399. https://doi.org/10.1128/AAC.01035-15.
10. Story-Roller E, Lamichhane G. 2018. Have we realized the full potential of β-lactams for treating drug-resistant TB? IUBMB Life 70:881–888. https://doi.org/10.1002/iub.1875.
11. Vora A, Tiwaskar M. 2022. Biapenem. J Assoc Physicians India 70:11–12.
12. Guo ZY, Zhao WJ, Zheng MQ, Liu S, Yan CX, Li P, Xu SF. 2019. Activities of biapenem against *Mycobacterium tuberculosis* in macrophages and mice. Biomed Environ Sci 32:235–241. https://doi.org/10.3967/bes2019.033.
13. Kaushik A, Ammerman NC, Tasneen R, Story-Roller E, Dooley KE, Dorman SE, Nuermberger EL, Lamichhane G. 2017. *In vitro* and *in vivo* activity of biapenem against drug-susceptible and rifampicin-resistant *Mycobacterium tuberculosis*. J Antimicrob Chemother 72:2320–2325. https://doi.org/10.1093/jac/dkx152.
14. Kaushik A, Makkar N, Pandey P, Parrish N, Singh U, Lamichhane G. 2015. Carbapenems and rifampin exhibit synergy against *Mycobacterium tuberculosis* and *Mycobacterium abscessus*. Antimicrob Agents Chemother 59:6561–6567. https://doi.org/10.1128/AAC.01158-15.
15. Sallusto F, Geginat J, Lanzavecchia A. 2004. Central memory and effector memory T cell subsets: function, generation, and maintenance. Annu Rev Immunol 22:745–763. https://doi.org/10.1146/annurev.immunol.22.012703.104702.
16. Cruz A, Torrado E, Carmona J, Fraga AG, Costa P, Rodrigues F, Appelberg R, Correia-Neves M, Cooper AM, Saraiva M, Pedrosa J, Castro AG. 2015. BCG vaccination-induced long-lasting control of *Mycobacterium tuberculosis* correlates with the accumulation of a novel population of $CD4^+IL\text{-}17^+TNF^+IL\text{-}2^+$ T cells. Vaccine 33:85–91. https://doi.org/10.1016/j.vaccine.2014.11.013.
17. Vogelzang A, Perdomo C, Zedler U, Kuhlmann S, Hurwitz R, Gengenbacher M, Kaufmann SHE. 2014. Central memory CD4+ T cells are responsible for the recombinant *Bacillus* Calmette-Guérin ΔureC::hly vaccine's superior protection against tuberculosis. J Infect Dis 210:1928–1937. https://doi.org/10.1093/infdis/jiu347.
18. Wang X, Zhang X, Zong Z, Yu R, Lv X, Xin J, Tong C, Hao Q, Qin Z, Xiong Y, Liu H, Ding G, Hu C, Biapenem Study Collaborative Group. 2013. Biapenem versus meropenem in the treatment of bacterial infections: a multicenter, randomized, controlled clinical trial. Indian J Med Res 138:995–1002.
19. Miller RA, Britigan BE. 1997. Role of oxidants in microbial pathophysiology. Clin Microbiol Rev 10:1–18. https://doi.org/10.1128/CMR.10.1.1.
20. Amaral EP, Conceição EL, Costa DL, Rocha MS, Marinho JM, Cordeiro-Santos M, D'Império-Lima MR, Barbosa T, Sher A, Andrade BB. 2016. N-acetyl-cysteine exhibits potent anti-mycobacterial activity in addition to its known anti-oxidative functions. BMC Microbiol 16:251. https://doi.org/10.1186/s12866-016-0872-7.
21. Aslan M, Ozben T. 2003. Oxidants in receptor tyrosine kinase signal transduction pathways. Antioxid Redox Signal 5:781–788. https://doi.org/10.1089/152308603770380089.
22. Poli G, Leonarduzzi G, Biasi F, Chiarpotto E. 2004. Oxidative stress and cell signalling. Curr Med Chem 11:1163–1182. https://doi.org/10.2174/0929867043365323.
23. Lee HM, Shin DM, Jo EK. 2009. *Mycobacterium tuberculosis* induces the production of tumor necrosis factor-α, interleukin-6, and CXCL8 in pulmonary epithelial cells through reactive oxygen species-dependent mitogen-activated protein kinase activation. J Bacteriol Virol 39:1–10. https://doi.org/10.4167/jbv.2009.39.1.1.
24. Ashwell JD. 2006. The many paths to p38 mitogen-activated protein kinase activation in the immune system. Nat Rev Immunol 6:532–540. https://doi.org/10.1038/nri1865.
25. Salvador JM, Mittelstadt PR, Guszczynski T, Copeland TD, Yamaguchi H, Appella E, Fornace AJ, Ashwell JD. 2005. Alternative p38 activation pathway

mediated by T cell receptor–proximal tyrosine kinases. Nat Immunol 6:390–395. https://doi.org/10.1038/ni1177.
26. Di Mitri D, Sambucci M, Loiarro M, De Bardi M, Volpe E, Cencioni MT, Gasperini C, Centonze D, Sette C, Akbar AN, Borsellino G, Battistini L. 2015. The p38 mitogen-activated protein kinase cascade modulates T helper type 17 differentiation and functionality in multiple sclerosis. Immunology 146:251–263. https://doi.org/10.1111/imm.12497.
27. Noubade R, Krementsov DN, Del Rio R, Thornton T, Nagaleekar V, Saligrama N, Spitzack A, Spach K, Sabio G, Davis RJ, Rincon M, Teuscher C. 2011. Activation of p38 MAPK in CD4 T cells controls IL-17 production and autoimmune encephalomyelitis. Blood 118:3290–3300. https://doi.org/10.1182/blood-2011-02-336552.
28. Alberts B, Johnson A, Lewis J, Raff M, Roberts K, Walter P. 2002. T cells and MHC proteins. Mol Biol Cell 4th Ed. Garland Science, New York NY.
29. Roche PA, Furuta K. 2015. The ins and outs of MHC class II-mediated antigen processing and presentation. Nat Rev Immunol 15:203–216. https://doi.org/10.1038/nri3818.
30. Kumar P. 2017. IFNγ-producing CD4+ T lymphocytes: the double-edged swords in tuberculosis. Clin Transl Med 6:21. https://doi.org/10.1186/s40169-017-0151-8.
31. Lyadova IV, Panteleev AV. 2015. Th1 and Th17 Cells in tuberculosis: protection, pathology, and biomarkers. Mediators Inflamm 2015:854507. https://doi.org/10.1155/2015/854507.
32. Ashenafi S, Aderaye G, Bekele A, Zewdie M, Aseffa G, Hoang ATN, Carow B, Habtamu M, Wijkander M, Rottenberg M, Aseffa A, Andersson J, Svensson M, Brighenti S. 2014. Progression of clinical tuberculosis is associated with a Th2 immune response signature in combination with elevated levels of SOCS3. Clin Immunol 151:84–99. https://doi.org/10.1016/j.clim.2014.01.010.
33. Dwivedi VP, Bhattacharya D, Chatterjee S, Prasad DVR, Chattopadhyay D, Van Kaer L, Bishai WR, Das G. 2012. *Mycobacterium tuberculosis* directs T helper 2 cell differentiation by inducing interleukin-1β production in dendritic cells. J Biol Chem 287:33656–33663. https://doi.org/10.1074/jbc.M112.375154.
34. Khader SA, Cooper AM. 2008. IL-23 and IL-17 in tuberculosis. Cytokine 41:79–83. https://doi.org/10.1016/j.cyto.2007.11.022.
35. Khader SA, Guglani L, Rangel-Moreno J, Gopal R, Junecko BAF, Fountain JJ, Martino C, Pearl JE, Tighe M, Lin Y-y, Slight S, Kolls JK, Reinhart TA, Randall TD, Cooper AM. 2011. IL-23 is required for long-term control of *Mycobacterium tuberculosis* and B cell follicle formation in the infected lung. J Immunol 187:5402–5407. https://doi.org/10.4049/jimmunol.1101377.
36. Fatima S, Kumari A, Dwivedi VP. 2021. Advances in adjunct therapy against tuberculosis: deciphering the emerging role of phytochemicals. MedComm (2020) 2:494–513. https://doi.org/10.1002/mco2.82.
37. Chatterjee S, Dwivedi VP, Singh Y, Siddiqui I, Sharma P, Van Kaer L, Chattopadhyay D, Das G. 2011. Early secreted antigen ESAT-6 of *Mycobacterium tuberculosis* promotes protective T helper 17 cell responses in a toll-like receptor-2-dependent manner. PLoS Pathog 7:e1002378. https://doi.org/10.1371/journal.ppat.1002378.
38. Azhar GS. 2012. DOTS for TB relapse in India: a systematic review. Lung India 29:147–153. https://doi.org/10.4103/0970-2113.95320.
39. Millet JP, Shaw E, Orcau À, Casals M, Miró JM, Caylà JA, Barcelona Tuberculosis Recurrence Working Group. 2013. Tuberculosis recurrence after completion treatment in a European city: reinfection or relapse? PLoS One 8:e64898. https://doi.org/10.1371/journal.pone.0064898.
40. Tousif S, Singh DK, Mukherjee S, Ahmad S, Arya R, Nanda R, Ranganathan A, Bhattacharyya M, Van Kaer L, Kar SK, Das G. 2017. Nanoparticle-formulated curcumin prevents posttherapeutic disease reactivation and reinfection with *Mycobacterium tuberculosis* following isoniazid therapy. Front Immunol 8:739. https://doi.org/10.3389/fimmu.2017.00739.
41. Seung KJ, Keshavjee S, Rich ML. 2015. Multidrug-resistant tuberculosis and extensively drug-resistant tuberculosis. Cold Spring Harb Perspect Med 5:a017863. https://doi.org/10.1101/cshperspect.a017863.
42. Guirado E, Schlesinger LS, Kaplan G. 2013. Macrophages in tuberculosis: friend or foe. Semin Immunopathol 35:563–583. https://doi.org/10.1007/s00281-013-0388-2.
43. Herb M, Schramm M. 2021. Functions of ROS in macrophages and antimicrobial immunity. Antioxidants 10:313. https://doi.org/10.3390/antiox10020313.
44. Schenk M, Fabri M, Krutzik SR, Lee DJ, Vu DM, Sieling PA, Montoya D, Liu PT, Modlin RL. 2014. Interleukin-1β triggers the differentiation of macrophages with enhanced capacity to present mycobacterial antigen to T cells. Immunology 141:174–180. https://doi.org/10.1111/imm.12167.
45. Cicchese JM, Evans S, Hult C, Joslyn LR, Wessler T, Millar JA, Marino S, Cilfone NA, Mattila JT, Linderman JJ, Kirschner DE. 2018. Dynamic balance of pro- and anti-inflammatory signals controls disease and limits pathology. Immunol Rev 285:147–167. https://doi.org/10.1111/imr.12671.
46. Winslow GM, Cooper A, Reiley W, Chatterjee M, Woodland DL. 2008. Early T-cell responses in tuberculosis immunity. Immunol Rev 225:284–299. https://doi.org/10.1111/j.1600-065X.2008.00693.x.
47. Lahey T, Sheth S, Matee M, Arbeit R, Horsburgh CR, Mtei L, Mackenzie T, Bakari M, Vuola JM, Pallangyo K, von Reyn CF. 2010. Interferon γ responses to mycobacterial antigens protect against subsequent HIV-associated tuberculosis. J Infect Dis 202:1265–1272. https://doi.org/10.1086/656332.
48. Szabo PA, Goswami A, Mazzuca DM, Kim K, O'Gorman DB, Hess DA, Welch ID, Young HA, Singh B, McCormick JK, Haeryfar SMM. 2017. Rapid and rigorous IL-17A production by a distinct subpopulation of effector memory T lymphocytes constitutes a novel mechanism of toxic shock syndrome immunopathology. J Immunol 198:2805–2818. https://doi.org/10.4049/jimmunol.1601366.
49. Lauvau G, Soudja SM. 2015. Mechanisms of memory T cell activation and effective immunity. Adv Exp Med Biol 850:73–80. https://doi.org/10.1007/978-3-319-15774-0_6.
50. Kumari A, Pahuja I, Negi K, Ghoshal A, Mukopadhyay S, Agarwal M, Mathew B, Maras JS, Chaturvedi S, Bhaskar A, Dwivedi VP. 2023. Withaferin a protects against primary and recurrent tuberculosis by modulating *Mycobacterium*-specific host immune responses. Microbiol Spectr 11:e0058323. https://doi.org/10.1128/spectrum.00583-23.
51. Pahuja I, Negi K, Kumari A, Agarwal M, Mukhopadhyay S, Mathew B, Chaturvedi S, Maras JS, Bhaskar A, Dwivedi VP. 2023. Berberine governs NOTCH3/AKT signaling to enrich lung-resident memory T cells during tuberculosis. PLoS Pathog 19:e1011165. https://doi.org/10.1371/journal.ppat.1011165.
52. Ahmad S, Bhattacharya D, Gupta N, Rawat V, Tousif S, Van Kaer L, Das G. 2020. Clofazimine enhances the efficacy of BCG revaccination via stem cell-like memory T cells. PLoS Pathog 16:e1008356. https://doi.org/10.1371/journal.ppat.1008356.